make contamination of F2 generation with males, leading to contamination of F2 hermaphrodites in step 68 with sperms from F2 males. The color phenotype should be suppressed in the crossed F1 progeny if the mutation is recessive. If all F1 males but not a hermaphrodite show the mutant phenotype, the gene is linked to X chromosome.

67| Transfer F1 hermaphrodites from step 66 to fresh 90-mm NGM plates. Culture at 20°C for 4-5 days. This step is to roughly synchronize the F2 generation in steps 66 and 67 so that the F2 worms can be easily discriminated from F3 generation by body size in step 68.

68| Pick single F2 gravid adult worms showing the mutant phenotype from the F1 pool plates from steps 66 and 67 and put into 10 µl of worm lysis solution. We use strips of 0.2-ml PCR tubes.

CRITICAL STEP Pick up gravid worms showing unambiguous mutant phenotype. Contamination of a heterozygous worm will significantly affect the reliability of mapping. Theoretically 3/16 of F2 worms will show color phenotype if recessive. Younger worms have less germline cells than gravid adults and the amount of their genomic DNA is insufficient for SNP typing of single worms. Note that mutant worms often grow significantly more slowly than siblings with heterozygous or wild-type background and may need more time to grow up to gravid adults.

69| Lyse the worms at 50°C for 60 min. Inactivate the lysis buffer at 83°C for 5 min. We program a PCR machine to carry out these incubations.

70| Add 30 µl TE and mix well by pipetting to prepare 40 µl worm lysate.

71| Repeat steps 64~70 to obtain enough single worm lysates form F2 with the phenotype. With >400 F2 lysates, the responsible region will be narrowed down to 1-2 Mb.

PAUSE POINT The single worm lysates can be stored at 4°C for weeks until use in the next steps.

72| Prepare a pool of the F2 lysates collected in steps 70~71. We collect 2 µl each from at least 48 single worm lysates. Steps 72~73 are not necessary if the gene of interest is found to be linked to X chromosome in steps 64~66.

73| Analyze one or two SNP(s) per chromosome of the pooled lysate to map the chromosome as described in BOX 2. Allele names, primers and restriction enzymes for typing the SNPs are listed in Table 5. Use N2 and CB4856 lysates as controls.

74| Analyze SNPs of individual worms by either restriction fragment length polymorphisms (RFLP) or direct sequencing of the PCR-amplified genomic fragments as described in BOX 2.

TROUBLESHOOTING

75| Amplify genomic fragments from candidate locus and sequence them to search for mutations. In most cases, mutations are found in exonic regions or splice sites. EMS treatment predominantly causes GC to AT transitions. Deletion of a short stretch also occurs at a lower frequency.

BOX 1| Testing resistance of bacterial clones to multiple antibiotics. TIMING 1~2 days

1. Draw a grid on the bottom surface of each LB agar plate containing a single or combinations of antibiotic(s). Label each square with clone numbers.

2. Pick up a single colony from a transformation plate with a single sterile micropipette tip and sequentially streak all the test plates with the tip in the squares assigned to the clone.

CRITICAL STEP The LB plate with the antibiotic(s) to which the clones are resistant should be streaked last; growth of the bacteria on the last, positive control plate in step 5 indicates that the other plates were also inoculated with enough amount of bacteria and incubated for

enough time.

3. Repeat step 2 to test the given number of clones.

4. Incubate all plates at 37°C for 8~12 hrs until the bacteria grow on the positive control plates.

5. Check growth of each clone on each plate to analyze resistance to the antibiotics.

6. Store the positive control plate with the grown bacteria as a master plate at 4°C for up to 1 month. The master plate is used to set up liquid cultures for plasmid preparation.

BOX 2| SNP Typing. TIMING 1~2 days

1. Synthesize SNP-typing primers for amplifying a genomic fragment.

2. Prepare the PCR mixture as tabulated below. We use BIOTAQ DNA Polymerase, but other proofreading polymerases may also be used.

Reagent	Amount per 10 µl reaction	Final concentration/amount
Single worm lysate (pool)	3 µl	3/40 worm
10 x NH4 buffer (Mg-free)	1 µl	1x
50 mM $MgCl_2$	0.5 µl	2.5 mM
2.5 mM each dNTP mixture	0.8 µl	0.2 mM each
1 µM each Primer Mixture	2 µl	0.2 µM each
BIOTAQ DNA Polymerase (5 u/µl)	0.1 µl	0.05 u/µl
DDW	2.6 µl	

CRITICAL STEP It is recommended to test several DNA polymerases available in each laboratory by typing SNPs of single N2 and CB4856 adult worms following the method described here before fixing DNA polymerase for SNP typing.

3. Run the PCR in a thermal cycler using the following parameters:

Cycle	Denature	Anneal	Extend
1	95°C, 3 min		
2 - 36	95°C, 40 sec	58°C, 40 sec	72°C, 40 sec
37			72°C, 7 min

4. Type the SNPs by either RFLP (A) or direct sequencing (B).

(A) SNP typing by RFLP.

(i) Premix the digestion mixture as tabulated below.

Reagent	Amount per reaction	Final concentration/amount
10 x restriction enzyme buffer	2.5 µl	1x
15% (w/v) sucrose/0.05% (w/v) Orange G	5 µl	3%/0.01%
Restriction Enzyme (8~20 u/µl)	0.5 µl	4~10 u
DDW	7 µl	

(ii) Add 15 µl digestion mixture to the PCR product from step 3 and mix by pipetting several times. Incubate at 37°C for >2 hour.

(iii) Run 10-µl aliquot of the digestion mixture on a 2% (w/v) SYNERGEL + 0.7% (w/v) agarose gel in Tris-borate-EDTA (TBE)

buffer. We use Electro-Fast Gel Systems for electrophoresis. A loading buffer is not required and the reaction mixture can be directly loaded.

TROUBLESHOOTING

(B) SNP typing by direct sequencing.

(i) Add 20 µl 1.5x DNA loading buffer to the PCR product.

(ii) Run 5-µl aliquot of the PCR mixture on a 1.5% (w/v) agarose gel to verify amplification.

TROUBLESHOOTING

(iii) Precipitate DNA by adding 3 µl 3 M NaOAc (pH5.2) and 100 µl ethanol to the remaining 25 µl PCR mixture.

(iv) Centrifuge the tubes at maximum speed for 10 min, rinse and dry the precipitate.

(v) Dissolve the precipitate in 30 µl TE and sequence with either of the SNP typing primers.

TIMING

Steps 1-16, Cloning genomic DNA fragment cassettes into Entry vectors: 2~3 weeks.

Step 17, Modification of genomic DNA fragment cassettes (Optional): 2~4 weeks.

Step 18(A), Constructing Destination vectors by inverse *attB*-PCR and BP cloning: 2~3 weeks.

Step 18(B), Constructing Destination vectors by ligating a promoter fragment to pDEST-PL vector: 2~3 weeks.

Steps 19-24, Constructing Expression clones: 1~2 weeks.

Steps 25-31, Generation of transgenic worms: 3~4 weeks.

Steps 32-43, Checking splicing patterns of mini-gene-derived mRNAs: 2~3 weeks.

Steps 44-45, Observation of cell-type-specific alternative splicing patterns: 2 days.

Steps 46-53, Integration of the extrachromosomal array: 3~4 weeks. For out-crossing the integrated line, it will take additional 3~4 days per generation.

Steps 54-63, Mutant screening: 3~4 weeks. For out-crossing the mutant line, it will take additional 3~7 days per generation.

Steps 64-75, SNP mapping and mutation search: 2~4 months.

BOX 1, Testing antibiotic-resistance: 1~2 days

BOX 2, SNP typing: 1~2 days

TROUBLESHOOTING

Step	Problem	Possible reason	Possible solution
12, 18A(xiii)	Few or no colonies obtained from BP reaction	Inappropriate primers	Make sure that each *att*B-flanked PCR primer is properly designed or selected.
		Inappropriate host strains	You must use DB3.1 or *ccd*B Survival competent cells in constructing Destination vectors.
21	Few or no colonies obtained from LR II Plus reaction.	Poor purity of plasmid DNAs	Purify mini-prep plasmid DNAs with a standard DNA purification column.
31	Little or no expression of fluorescent proteins	Low expression levels	If you obtain many marker-positive and non-fluorescent transgenic lines, check expression levels as described in steps 32-43. If the mRNA was not detected, Try other promoters to drive the mini-genes.
		mRNAs are degraded by NMD.	Check the design of the mini-genes, and reconstruct new mini-genes.
		Aberrant splicing of the mini-gene-derived mRNAs	Check splicing patterns of the mini-gene-derived mRNAs as described in steps 32-43. Genomic fragments inserted in the mini-genes usually undergo proper splicing. If you detect aberrant splicing, trim the genomic fragment (steps 1-16) or remove the cryptic splice sites by site-directed mutagenesis (step 17).
		Aberrant translation of the mini-gene-derived mRNAs	Check expression of the fluorescent proteins by Western Blotting with anti-GFP and/or anti-RFP antibodies. If you detect expected mRNAs but few proteins, optimize the preferred initiation codons and remove unnecessary ATGs out of frame.
		Aberrant folding or instability of the fluorescent proteins	N-terminal tags such as GST may improve the expression of the reporter. Repeated trial and error may be required to establish a reporter reflecting the alternative splicing pattern of the endogenous gene.
53	No integrant line	Low efficiency in integrant	Use extrachromosomal lines with lower transmission rate, and it

	obtained	screening	will be easier to distinguish integrated lines from parental lines. Irradiate as many fluorescent worms as possible and isolate as many uniformly fluorescent F1 worms as possible.
63	No mutant lines established	Sterility or lethality of the mutant	If you find sterile or arrested F2 worms with apparent color phenotypes, try mutagenesis with reporter heterozygotes or extrachromosomal lines. If you find dead F2 embryos with apparent colors, the regulator may be essential. You may establish weaker alleles in further screening.
		Inappropriate screening strategy	If you do not find any F2 worms with aberrant color phenotypes, reconsider the screening strategies, e.g. the tissues where the reporter is expressed or the structures of the reporter mini-genes.
74	Responsible locus cannot be narrowed down	Inappropriate crossing or ambiguous F2 phenotypes	Make sure that you pooled crossed F1 progeny in step 66. Make sure that you collected single worm lysates from F2 hermaphrodites showing the mutant phenotype in step 68.
		The responsible gene may be within a rearranged region	It is important to outcross the integrated reporter lines before mutagenesis. Use other integrated alleles for mutagenesis.
		The responsible gene is close to the locus of the integrated reporter	Use other integrated alleles for mutagenesis.
BOX 2-4(A)(iii), -4(B)(ii)	No or little amplification of genomic fragments by PCR	The isolated F2 worms are too young	Collect single worm lysates from gravid F2 hermaphrodites. Mixing of lysates in step 70 may be insufficient.
	Ambiguous pattern of RFLP or sequencing.	Contamination of the F2 hermaphrodites collected in step 68 with sperms from F2 males.	Pool the F1 hermaphrodites at L4 stage in step 66.

ANTICIPATED RESULTS

Here we summarize our success rate of each step in mini-gene construction. In amplifying genomic DNA fragments for cloning the genomic fragment cassettes in Entry vectors, most of the fragments were <3 kb and were specifically amplified from N2 genomic DNA (steps 1~7). These *att*B-PCR products were successfully cloned by BP II reaction (steps 10~16), although the probability of clones carrying the correct insert varies from 10% to 90% probably due to variable amount of co-amplified non-specific PCR products. Sometimes we found that the genomic DNA sequences of the N2 worms in our laboratory are different from the reference N2 genomic DNA sequences in GenBank/EMBL/DDBJ databases (Acc. No. NC_003279~NC_003284). We reasoned this is due to mis-calling in the sequencing process of the reference or to spontaneous mutations during the maintenance of the strain, and we use the fragments as they are. Site-directed mutagenesis (step 17) is achieved with 60%~80% of the success rate, although 10~30% of the clones contain errors in the oligo DNA sequences. Construction of Destination vectors by inverse *att*B-PCR (step 18A) is less efficient; the rate of the correct clones is <10%~30%. Therefore, specific amplification of the vector fragment (steps 18A(i)~(iv)) and pre-screening by antibiotic-resistance (steps 18A(xiii)~(xiv)) are important for higher success probability. Assembling the mini-genes by LR II Plus reaction (steps 19~24) is efficient; 60%~90% of the carbenicillin-resistant clones in step 21 carry the correct expression constructs. We have not experienced sequence modification in the *att*B homologous recombination sites or in the inserts by the LR II Plus reaction.

Construction of the fluorescence reporter mini-genes (steps 1~24), generation of the transgenic worm lines (steps 25~31) and imaging of the fluorescent reporter worms (steps 44~45) should provide data on the spatiotemporal distribution of alternative splicing events in living worms. We usually use ubiquitous or broadly-expressing promoters first to outline expression profiles in *vivo*. In most cases, each tissue expresses either or both of the fluorescent proteins. In some cases of mutually exclusive alternative splicing reporters, however, expression of the fluorescent proteins was not detected in certain tissues, probably due to double inclusion or double skipping of the alternative exons. We narrow down tissues where the fluorescence reporter mini-genes are driven in further genetic analyses as described below.

It is recommended to confirm that the expression profile of the alternative splicing reporter is consistent with that of the endogenous gene. In the case of the *egl-15* gene [26], there was a genetic evidence that *egl-15(5A)* isoform specifically functions in sex myoblasts that differentiate into vulval muscles in hermaphrodites [49]. We confirmed that vulval muscles properly expressed exon 5A-RFP isoform of the *egl-15* reporter, and the reporter showed muscle-specificity when expressed under various tissue-specific promoters [26]. In the case of the *lethal* (*let*)-*2* gene, previous promoter analysis had demonstrated that *let-2* is expressed in the body wall muscles and two distal tip cells (DTCs) [50]. As the number and total mass of the body wall muscles are much more than those of the DTCs, we reasoned that developmentally regulated switching of the *let-2* alternative splicing [51] occurs in body wall muscles. When the *let-2* reporter was expressed under a ubiquitous promoter, all the tissues expressed the embryonic form (GFP) in embryos and young larvae, while only the body wall muscles turned the reporter expression to the adult form (RFP) during development (Figure 4a), suggesting the presence of tissue-specific and developmental regulation in this event. By utilizing a body wall muscle-specific promoter, we successfully visualized the developmental switching as shown in the previous study [27] and in Figure 4b. In cases of alternative splicing events whose spatiotemporal distributions are unknown, expression profiles of the fluorescence splicing reporter may be confirmed when mutants isolated by the phenotype in the reporter expression also show the same defect in the splicing pattern of the endogenous gene.

In the screening for mutants defective in the muscle-specific expression of the *egl-15* reporter, we utilized the color of the body wall muscles [26], although expression of the endogenous *egl-15* gene was hardly detected in the body wall muscles [52]. We pooled about three

hundred P0 worms in total in two independent screening using two independent integrated alleles. We isolated fifteen *alternative splicing defective* (*asd*)-*1* and ten *suppressor* (*sup*)-*12* alleles [26,28]. The number of *asd-1* alleles was more than expected, and we reasoned that *asd-1* null mutants are viable and ASD-1 coding region has many CAA and CAG codons, encoding glutamine, which turn into nonsense codons TAA and TAG by EMS treatment [26]. Although the *sup-12* null mutants are sterile in the *egl-15* reporter-homozygous background, we successfully established the *sup-12* alleles in the reporter heterozygous background [28]. Various missense mutations in the RNA-binding domain of SUP-12 caused weaker color phenotypes, suggesting involvement of these residues in RNA-binding [28]. ASD-1 and SUP-12, isolated in this way, turned out to be involved in the regulation of the endogenous *egl-15* gene in the vulval muscles[26,28].

In the screening for mutants of the *let-2* reporter expression, we mutagenized an integrated allele expressing the *let-2* reporter only in the body wall muscles. We utilized an epifluorescence dissection microscope MZ16FA and a dual band-pass filter set and successfully isolated six *asd-2* mutant alleles, all of which remain expressing the embryonic form (GFP) in adulthood (Figure 4c). In search for *cis*-elements involved in the ASD-2-mediated regulation, we disrupted CTAAC repeats in intron 10 of the pair of the *let-2* reporter mini-genes, since the repeats almost matched the bipartite consensus sequence for QKI [53], a mammalian homolog of ASD-2. The mutant *let-2* reporter showed the same phenotype as the *asd-2* mutants and recombinant ASD-2 protein specifically bound to the CUAAC repeats *in vitro* [27]. Furthermore, the mutant *let-2* reporter no longer responded to overexpression of ASD-2, confirming that ASD-2 functions via binding to the CUAAC repeats [27].

Despite our accumulating experience, about half of the fluorescence alternative splicing reporters we generated showed little or no fluorescence. In most of them, the alternative exons themselves encode hydrophobic stretches and this property may have caused aggregation or affected folding of the fluorescent proteins. For the rest, the transcripts from the reporter were not detected and we could not specify the reason for that. We are therefore focusing on the reporters that work well.

Author contributions

H.K. designed and performed experiments, and wrote the manuscript; G.O., H.S. and H.M. designed and performed experiments to improve the procedure; M.H. organized the study.

ACKNOWLEDGMENTS

We thank the present and past members of Masatoshi Hagiwara lab for their suggestions. We thank Masayuki Hagiwara, Hajime Ito, Yuriko Kikuchi, Takayuki Yamada and Kohtaro Kawamata for technical assistance. We thank CGC for strains. We acknowledge support from grants from the Ministry of Education, Culture, Sports, Science and Technology (MEXT), Japan Society for the Promotion of Science (JSPS) and Japan Science and Technology Agency (JST).

Competing financial interests

The authors declare that they have no competing financial interests.

Figure legends

Figure 1| Schematic structure of fluorescence reporter mini-genes and expected mRNA isoforms.
Two-construct fluorescence alternative splicing reporter mini-genes for mutually exclusive exons **(a)** and a cassette exon **(b)**. Boxes indicate exons. 'a' and 'b', mutually exclusive exons; 'c', a cassette exon. Genomic fragments to be analyzed are colored in orange. GFP and RFP cDNAs are in green and magenta, respectively. Green circles and red diamonds indicate artificially introduced translation initiation codons and termination codons, respectively. Open reading frames are colored; GFP-fusion proteins, RFP-fusion proteins and non-fluorescent proteins are in green, magenta and cyan, respectively. See text for details.

Figure 2| Strategies for constructing fluorescence alternative splicing reporter mini-genes by site-directed recombination.
(a) Schematic diagram of construction of the reporter mini-genes by site-directed LR recombination between a Destination and two Entry vectors. The Destination vector provides a promoter and a 3' cassette. The Entry vectors provide a genomic fragment cassette and a fluorescent protein cassette. **(b)** Schematic diagram of the strategy for constructing a genomic fragment cassette in pENTR-L1-R5 Entry vector. A genomic fragment of interest is amplified with a GSP-*att*B primer set and an *att*B-adapter primer set in a 2-step PCR and subcloned in the Entry vector by site-directed BP recombination. A modification is optionally introduced into the genomic fragment by site-directed mutagenesis. **(c)** Schematic diagram of the strategy for constructing Destination vectors by inverse *attB*-PCR and site-directed BP recombination. A vector fragment is amplified with a VSP-*att*B primer set and an *att*B-adapter primer set in a 2-step PCR and converted to the Destination vector by site-directed BP recombination.

Figure 3| Schematic structure of pDEST-PL.
pDEST-PL was converted from pPD49.26 [39] and has a multicloning site (MCS), synthetic intron/exon structure, a Destination vector cassette and a 3' cassette derived from the *unc-54* gene. The MCS can be used for subcloning a promoter fragment. Unique restriction sites in the MCS are indicated. H, *Hin* dIII; Sph, *Sph* I; Xb, *Xba*I.

Figure 4| Visualizing developmental switching of the mutually exclusive exons of the *let-2* gene.
The schematic structure of the *let-2* mutually exclusive alternative splicing reporter mini-genes [27] are shown in Figure 1a; expression of GFP indicates selection of embryonic exon 9 and expression of RFP indicates selection of adult exon 10. **(a)** Confocal images of transgenic worms expressing the *let-2* reporter under a broadly-expressing promoter. (Left) Exon 9-GFP, (middle) Exon 10-RFP, (right) Merged view. Note that all tissues in embryos (thin arrows, Emb) and an L1 larva (large arrow, L1) exclusively express exon 9-GFP, while body wall muscles (bwm), pharynx (phx) and vulval muscles (vm) come to express exon 10-RFP in an adult. The images were acquired with a laser scanning confocal microscope Fluoview 500 (Olympus). **(b, c)** Microphotographs of transgenic worms expressing the *let-2* reporter under a body wall muscle-specific promoter in the wild-type **(b)** and *asd-2* mutant **(c)** backgrounds. Note that the body wall muscles in the *asd-2* mutant worms fail to switch from exon 9-GFP to exon 10-RFP during larval development. The images were acquired with an epifluorescence dissection microscope MZ16FA (Leica) equipped with a dual band-pass filter set GFP/DsRed (chroma), and a color cooled CCD camera DP71 (Olympus). Scale bars, 100 μm.

Tables

Table 1. Entry vectors for fluorescent proteins.

Vector Name	Description
pENTR-L5-ECFP-L2	cyan
pENTR-L5-EGFP-L2	green
pENTR-L5-HcRed-L2	red
pENTR-L5-mRFP-L2	red
pENTR-L5-Venus-L2	yellow
pENTR L5-(-1)EGFP-L2	frame-shift
pENTR L5-(+1)EGFP-L2	frame-shift
pENTR L5-(-1)mRFP-L2	frame-shift
pENTR L5-(+1)mRFP-L2	frame-shift

Sequence information of these vectors is available in Supplementary Sequence Archive. Further information about these vectors is available upon request to H.K.

Table 2. Destination vectors for expression in *C. elegans*.

Vector Name	Description
pDEST-PL	promoter-less
pDEST-aex-3p	pan-neuronal
pDEST-che-2p	amphid sensory neurons
pDEST-dpy-7p	hypodermal cells
pDEST-eat-4p	glutamatergic neurons
pDEST-eft-3p	ubiquitous
pDEST-elt-2p	intestine
pDEST-F25B3.3p	pan-neuronal
pDEST-ges-1p	intestine
pDEST-gon-2p	intestine
pDEST-gst-42p	intestine
pDEST-gtl-1p	intestine
pDEST-hsp16-2p	heat-shock-inducible
pDEST-hsp16-41p	heat-shock-inducible
pDEST-mec-7p	touch receptor neurons
pDEST-myo-2p	pharyngeal muscles
pDEST-myo-3p	body wall muscles, vulval muscles
pDEST-sdf-9p	XXXL/R
pDEST-unc-4p	subset of motor neurons DA, VA, VC, SAB

These vectors are available upon request to H.K..

Table 3. Sequences of primers used for constructing genomic DNA fragment cassettes in Entry vectors.

Primer	Sequence	Use
GSP-*att*B1F	5′-AA AAA GCA GGC TCC ACC ATG G -(gene-specific sequence)-3′	Steps 2, 41
GSP-*att*B5R	5′-T ATA CAA AGT TGT -(gene-specific sequence)-3′	Step 2
*att*B1adapterF	5′-GGGG ACAAGTTTGTACAAAAAAGCAGGCT-3′	Steps 5, 41
*att*B5adapterR	5′-GGGG ACAACTTTTGTATACAAAGTTG-3′	Step 5

Single underlines indicate 12 bases of the *att*B sequences included in the GSPs.

Double underline indicates Kozak's consensus sequence that allows efficient translation initiation in higher eukaryotic cells.

Table 4. Sequences of primers used for constructing Destination vectors by inverse *att*B-PCR.

Primer	Sequence	Use
VSP-*att*B1R	5′- GTA CAA ACT TGT G -(template-specific sequence)-3′	Step18A(ii)
VSP-*att*B2F	5′- G TAC AAA GTG GTC -(template-specific sequence)-3′	Step18A(ii)
*att*B1adapterR	5′- GGGG AGCCTGCTTTTTTGTACAAACTTGT G -3′	Step18A(v)
*att*B2adapterF	5′- GGGG ACCCAGCTTTCTTGTACAAAGTGGT C -3′	Step18A(v)

Underlines indicate 12 bases of the *att*B sequences included in the VSPs.

Table 5. SNPs for mapping genes to chromosomes.

Chromosome	allele	Primers	Restriction Enzyme
I	pkP1101	CGCGTTTCGTAATGTATCG	*Eco* RI
		GAACTTCCAGGTCACTCTGG	
I	pkP1119	CTCCATTTTGGAACTCCCAG	*Eco* RI
		TCAAATTTGGCACGTCATCAG	
II	pkP2107	TCCACACTATTTCCCTCGTG	*Dra* I
		GAGCAATCAAGAACCGGATC	
III	pkP3093	CGCTGAAATTGAGGAGCAG	*Ava* II
		TGGGCTTAACAATGATGGG	
III	pkP3102	CATTAGGAAGTGATGCAAGTGG	*Ava* II
		TGGATTTGAGAGGTGTCCATAG	
IV	pkP4071	CCAAACAACCTACAGAAAATGC	*Dra* I
		AAGATATTCATGCGTCGTAGTG	
V	pkP5076	CGGAAAATTGCGACTGTC	*Dra* I
		ATTAGGACTGCTTGGCTTCC	
V	pkP5097	TAGTGTTCATAGCATCCCATTG	*Dra* I
		GTGCTAATTCCAGAAATGATCC	

References

1. Wang, E.T., Sandberg, R., Luo, S., Khrebtukova, I., Zhang, L., Mayr, C., Kingsmore, S.F., Schroth, G.P., and Burge, C.B. Alternative isoform regulation in human tissue transcriptomes. *Nature* **456**, 470-476 (2008).
2. Matlin, A.J., Clark, F., and Smith, C.W. Understanding alternative splicing: towards a cellular code. *Nat Rev Mol Cell Biol* **6**, 386-398 (2005).
3. Black, D.L. Mechanisms of alternative pre-messenger RNA splicing. *Annu Rev Biochem* **72**, 291-336 (2003).
4. Jin, Y., Suzuki, H., Maegawa, S., Endo, H., Sugano, S., Hashimoto, K., Yasuda, K., and Inoue, K. A vertebrate RNA-binding protein Fox-1 regulates tissue-specific splicing via the pentanucleotide GCAUG *Embo J* **22**, 905-912 (2003).
5. Jensen, K.B., Dredge, B.K., Stefani, G., Zhong, R., Buckanovich, R.J., Okano, H.J., Yang, Y.Y., and Darnell, R.B. Nova-1 regulates neuron-specific alternative splicing and is essential for neuronal viability. *Neuron* **25**, 359-371 (2000).
6. Ladd, A.N., Charlet, N., and Cooper, T.A. The CELF family of RNA binding proteins is implicated in cell-specific and developmentally regulated alternative splicing. *Mol Cell Biol* **21**, 1285-1296 (2001).
7. Sheives, P. and Lynch, K.W. Identification of cells deficient in signaling-induced alternative splicing by use of somatic cell genetics. *RNA* **8**, 1473-1481 (2002).
8. Wang, Z., Rolish, M.E., Yeo, G, Tung, V., Mawson, M., and Burge, C.B. Systematic identification and analysis of exonic splicing silencers. *Cell* **119**, 831-845 (2004).
9. Ellis, P.D., Smith, C.W., and Kemp, P. Regulated tissue-specific alternative splicing of enhanced green fluorescent protein transgenes conferred by alpha-tropomyosin regulatory elements in transgenic mice. *J Biol Chem* **279**, 36660-36669 (2004).
10. Oltean, S., Sorg, B.S., Albrecht, T., Bonano, V.I., Brazas, R.M., Dewhirst, M.W., and Garcia-Blanco, M.A. Alternative inclusion of fibroblast growth factor receptor 2 exon IIIc in Dunning prostate tumors reveals unexpected epithelial mesenchymal plasticity. *Proc Natl Acad Sci U S A* **103**, 14116-14121 (2006).
11. Levinson, N., Hinman, R., Patil, A., Stephenson, C.R., Werner, S., Woo, G.H., Xiao, J., Wipf, P., and Lynch, K.W. Use of transcriptional synergy to augment sensitivity of a splicing reporter assay. *RNA* **12**, 925-930 (2006).
12. MacMorris, M.A., Zorio, D.A., and Blumenthal, T. An exon that prevents transport of a mature mRNA. *Proc Natl Acad Sci U S A* **96**, 3813-3818 (1999).
13. Newman, E.A., Muh, S.J., Hovhannisyan, R.H., Warzecha, C.C., Jones, R.B., McKeehan, W.L., and Carstens, R.P. Identification of RNA-binding proteins that regulate FGFR2 splicing through the use of sensitive and specific dual color fluorescence minigene assays. *RNA* **12**, 1129-1141 (2006).
14. Orengo, J.P., Bundman, D., and Cooper, T.A. A bichromatic fluorescent reporter for cell-based screens of alternative splicing. *Nucleic Acids Res* **34**, e148 (2006).
15. Warzecha, C.C., Sato, T.K., Nabet, B., Hogenesch, J.B., and Carstens, R.P. ESRP1 and ESRP2 are epithelial cell-type-specific regulators of FGFR2 splicing. *Mol Cell* **33**, 591-601 (2009).
16. Oltean, S., Febbo, P.G, and Garcia-Blanco, M.A. Dunning rat prostate adenocarcinomas and alternative splicing reporters: powerful tools to study epithelial plasticity in prostate tumors in vivo. *Clin Exp Metastasis* **25**, 611-619 (2008).

17. Stoilov, P., Lin, C.H., Damoiseaux, R., Nikolic, J., and Black, D.L. A high-throughput screening strategy identifies cardiotonic steroids as alternative splicing modulators. *Proc Natl Acad Sci U S A* **105**, 11218-11223 (2008).
18. Bonano, V.I., Oltean, S., and Garcia-Blanco, M.A. A protocol for imaging alternative splicing regulation *in vivo* using fluorescence reporters in transgenic mice. *Nat Protoc* **2**, 2166-2181 (2007).
19. Bonano, V.I., Oltean, S., Brazas, R.M., and Garcia-Blanco, M.A. Imaging the alternative silencing of *FGFR2* exon IIIb *in vivo*. *RNA* **12**, 2073-2079 (2006).
20. Takeuchi, A., Hosokawa, M., Nojima, T., and Hagiwara, M. Splicing Reporter Mice Revealed the Evolutionally Conserved Switching Mechanism of Tissue-Specific Alternative Exon Selection. *PLoS One* (in press).
21. Zahler, A.M. Alternative splicing in *C. elegans*. In *WormBook - Molecular biology -*, (eds. Blumenthal, T.) 1-13 (2005).
22. Spike, C.A., Davies, A.G, Shaw, J.E., and Herman, R.K. MEC-8 regulates alternative splicing of *unc-52* transcripts in *C. elegans* hypodermal cells. *Development* **129**, 4999-5008 (2002).
23. Spartz, A.K., Herman, R.K., and Shaw, J.E. SMU-2 and SMU-1, *Caenorhabditis elegans* homologs of mammalian spliceosome-associated proteins RED and fSAP57, work together to affect splice site choice. *Mol Cell Biol* **24**, 6811-6823 (2004).
24. Spike, C.A., Shaw, J.E., and Herman, R.K. Analysis of *smu-1*, a gene that regulates the alternative splicing of *unc-52* pre-mRNA in *Caenorhabditis elegans*. *Mol Cell Biol* **21**, 4985-4995 (2001).
25. Kabat, J.L., Barberan-Soler, S., McKenna, P., Clawson, H., Farrer, T., and Zahler, A.M. Intronic alternative splicing regulators identified by comparative genomics in nematodes. *PLoS Comput Biol* **2**, e86 (2006).
26. Kuroyanagi, H., Kobayashi, T., Mitani, S., and Hagiwara, M. Transgenic alternative-splicing reporters reveal tissue-specific expression profiles and regulation mechanisms *in vivo*. *Nat Methods* **3**, 909-915 (2006).
27. Ohno, G, Hagiwara, M., and Kuroyanagi, H. STAR family RNA-binding protein ASD-2 regulates developmental switching of mutually exclusive alternative splicing *in vivo*. *Genes Dev* **22**, 360-374 (2008).
28. Kuroyanagi, H., Ohno, G, Mitani, S., and Hagiwara, M. The Fox-1 family and SUP-12 coordinately regulate tissue-specific alternative splicing *in vivo*. *Mol Cell Biol* **27**, 8612-8621 (2007).
29. Lander, E.S., Linton, L.M., Birren, B. et al. Initial sequencing and analysis of the human genome. *Nature* **409**, 860-921 (2001).
30. David, C.J. and Manley, J.L. The search for alternative splicing regulators: new approaches offer a path to a splicing code. *Genes Dev* **22**, 279-285 (2008).
31. Kuroyanagi, H. Fox-1 family of RNA-binding proteins. *Cell Mol Life Sci* **66**, 3895-3907 (2009).
32. Mello, C.C., Kramer, J.M., Stinchcomb, D., and Ambros, V. Efficient gene transfer in *C.elegans*: extrachromosomal maintenance and integration of transforming sequences. *EMBO J* **10**, 3959-3970 (1991).
33. Van Buskirk, C. and Sternberg, P.W. Epidermal growth factor signaling induces behavioral quiescence in *Caenorhabditis elegans*. *Nat Neurosci* **10**, 1300-1307 (2007).
34. Chang, Y.F., Imam, J.S., and Wilkinson, M.F. The nonsense-mediated decay RNA surveillance pathway. *Annu Rev Biochem* **76**, 51-74 (2007).
35. Isken, O. and Maquat, L.E. Quality control of eukaryotic mRNA: safeguarding cells from abnormal mRNA function. *Genes Dev* **21**, 1833-1856 (2007).
36. Pulak, R. and Anderson, P. mRNA surveillance by the *Caenorhabditis elegans smg* genes. *Genes Dev* **7**, 1885-1897 (1993).

37. Burgess, R.R. Use of bioinformatics in planning a protein purification. *Methods Enzymol* **463**, 21-28 (2009).
38. Brondyk, W.H. Selecting an appropriate method for expressing a recombinant protein. *Methods Enzymol* **463**, 131-147 (2009).
39. Mello, C.C. and Fire, A. DNA Transformation. In *Caenorhabditis elegans: Modern Biological Analysis of an Organism*, (eds. Epstein, H. F. and Shakes, D. C.) 452-482 (Academic Press, Inc., San Diego, CA, USA, 1995).
40. Clark, S.G., Lu, X., and Horvitz, H.R. The *Caenorhabditis elegans* locus *lin-15*, a negative regulator of a tyrosine kinase signaling pathway, encodes two different proteins. *Genetics* **137**, 987-997 (1994).
41. Mitani, S. Genetic regulation of *mec-3* gene expression implicated in the specification of the mechanosensory neuron cell types in *Caenorhabditis elegans*. *Dev. Growth & Diff.* **37**, 551-557 (1995).
42. Caceres, J.F. and Kornblihtt, A.R. Alternative splicing: multiple control mechanisms and involvement in human disease. *Trends Genet* **18**, 186-193 (2002).
43. Wicks, S.R., Yeh, R.T., Gish, W.R., Waterston, R.H., and Plasterk, R.H. Rapid gene mapping in *Caenorhabditis elegans* using a high density polymorphism map. *Nat Genet* **28**, 160-164 (2001).
44. Ryder, S.P., Recht, M.I., and Williamson, J.R. Quantitative analysis of protein-RNA interactions by gel mobility shift. In *Methods Mol Biol* 99-115 (2008).
45. Clarke, P.A. Labeling and Purification of RNA Synthesized by In Vitro Transcription. In *RNA-Protein Interaction Protocols*, (eds. Haynes, S. R.) 1-10 (Humana Press Inc., Totowa, New Jersey, USA, 1999).
46. Ohno, M. and Shimura, Y. Nuclear cap binding protein from HeLa cells. *Methods Enzymol* **181**, 209-215 (1990).
47. Johnstone, I.L. Molecular Biology. In *C. elegans A Practical Approach*, (eds. Hope, I. A.) 201-225 (Oxford University Press, New York, New York, USA, 1999).
48. Inoue, H., Nojima, H., and Okayama, H. High efficiency transformation of *Escherichia coli* with plasmids. *Gene* **96**, 23-28 (1990).
49. Goodman, S.J., Branda, C.S., Robinson, M.K., Burdine, R.D., and Stern, M.J. Alternative splicing affecting a novel domain in the *C. elegans* EGL-15 FGF receptor confers functional specificity. *Development* **130**, 3757-3766 (2003).
50. Graham, P.L., Johnson, J.J., Wang, S., Sibley, M.H., Gupta, M.C., and Kramer, J.M. Type IV collagen is detectable in most, but not all, basement membranes of *Caenorhabditis elegans* and assembles on tissues that do not express it. *J Cell Biol* **137**, 1171-1183 (1997).
51. Sibley, M.H., Johnson, J.J., Mello, C.C., and Kramer, J.M. Genetic identification, sequence, and alternative splicing of the *Caenorhabditis elegans* alpha 2(IV) collagen gene. *J Cell Biol* **123**, 255-264 (1993).
52. Kostas, S.A. and Fire, A. The T-box factor MLS-1 acts as a molecular switch during specification of nonstriated muscle in *C. elegans*. *Genes Dev* **16**, 257-269 (2002).
53. Galarneau, A. and Richard, S. Target RNA motif and target mRNAs of the Quaking STAR protein. *Nat Struct Mol Biol* **12**, 691-698 (2005).

⌘ Author's Choice

THE JOURNAL OF BIOLOGICAL CHEMISTRY VOL. 285, NO. 8, pp. 5532–5540, February 19, 2010

Regulation of Vascular Endothelial Growth Factor (VEGF) Splicing from Pro-angiogenic to Anti-angiogenic Isoforms

*A NOVEL THERAPEUTIC STRATEGY FOR ANGIOGENESIS**

Received for publication, October 13, 2009 Published, JBC Papers in Press, November 11, 2009, DOI 10.1074/jbc.M109.074930

Dawid G. Nowak[‡1], Elianna Mohamed Amin[§1], Emma S. Rennel[‡], Coralie Hoareau-Aveilla[‡], Melissa Gammons[‡], Gopinath Damodoran[‡], Masatoshi Hagiwara[¶], Steven J. Harper[‡], Jeanette Woolard[‡2], Michael R. Ladomery[§2,3], and David O. Bates[‡2,4]

From the [‡]Microvascular Research Laboratories, Bristol Heart Institute, Department of Physiology and Pharmacology, School of Veterinary Sciences, University of Bristol, Bristol BS2 8EJ, United Kingdom, the [§]Centre for Research in Biomedicine, School of Life Sciences, University of the West of England, Bristol BS16 1QY, United Kingdom, and the [¶]Department of Genetics, University of Tokyo Medical and Dental School, Tokyo 113-8510, Japan

Vascular endothelial growth factor (VEGF) is produced either as a pro-angiogenic or anti-angiogenic protein depending upon splice site choice in the terminal, eighth exon. Proximal splice site selection (PSS) in exon 8 generates pro-angiogenic isoforms such as $VEGF_{165}$, and distal splice site selection (DSS) results in anti-angiogenic isoforms such as $VEGF_{165}b$. Cellular decisions on splice site selection depend upon the activity of RNA-binding splice factors, such as ASF/SF2, which have previously been shown to regulate VEGF splice site choice. To determine the mechanism by which the pro-angiogenic splice site choice is mediated, we investigated the effect of inhibition of ASF/SF2 phosphorylation by SR protein kinases (SRPK1/2) on splice site choice in epithelial cells and in *in vivo* angiogenesis models. Epithelial cells treated with insulin-like growth factor-1 (IGF-1) increased PSS and produced more $VEGF_{165}$ and less $VEGF_{165}b$. This down-regulation of DSS and increased PSS was blocked by protein kinase C inhibition and SRPK1/2 inhibition. IGF-1 treatment resulted in nuclear localization of ASF/SF2, which was blocked by SPRK1/2 inhibition. Pull-down assay and RNA immunoprecipitation using VEGF mRNA sequences identified an 11-nucleotide sequence required for ASF/SF2 binding. Injection of an SRPK1/2 inhibitor reduced angiogenesis in a mouse model of retinal neovascularization, suggesting that regulation of alternative splicing could be a potential therapeutic strategy in angiogenic pathologies.

Vascular endothelial growth factor (VEGF-A, hereafter referred to as VEGF)[5] is a key regulatory component in physiological and pathological angiogenesis. Inhibition of VEGF has shown to be effective in cancer (1) and ocular angiogenesis (2), and it is up-regulated by a number of growth factors also implicated in these conditions, including insulin-like growth factor-1 (IGF-1) (3). VEGF is generated as multiple isoforms by alternative splicing (4). There are two principal families of VEGF isoforms, the pro-angiogenic $VEGF_{xxx}$ isoforms, generated by proximal splice site selection in the terminal exon, exon 8a (5), and the anti-angiogenic $VEGF_{xxx}b$ isoforms (6), generated by use of a distal splice site 66 bp further into exon 8, generating mRNA isoforms that contain exon 8b. As the stop codon for the protein is encoded in exon 8, these two isoforms contain alternate six amino acids at the C terminus (Fig. 1*A*). The pro-angiogenic isoforms such as $VEGF_{165}$ encode a terminal six amino acid sequence of CDKPRR, and the anti-angiogenic isoforms such as $VEGF_{165}b$ encode SLTRKD (7). Many normal tissues, including the eye generate both isoforms (8), and previous studies have shown that the anti-angiogenic isoforms dominate in non-angiogenic tissues such as the normal colon (9) and the vitreous (8). However, there is a splicing switch in angiogenic conditions such as proliferative diabetic retinopathy (8), colon (9), prostate (10), renal (7), and skin cancers (11), and in Denys Drash Syndrome (12). In contrast, in non-angiogenic conditions where VEGF is up-regulated, such as glaucoma and rhegmatogenous retinal detachment associated with proliferative vitreoretinopathy (13) or glaucoma (14), the anti-angiogenic isoforms are up-regulated. We have previously shown that IGF-1 can switch splicing in cultured epithelial cells from anti-angiogenic to pro-angiogenic isoforms (15). As IGF-1 has been implicated in a number of angiogenic conditions including diabetic retinopathy and colon cancer, we hypothesized that the mechanism through which IGF-1 mediates this change in splicing may be a potential therapeutic target to prevent angiogenesis. To this end, we have investigated the signaling pathways, the splicing factors involved, and the possibility of therapeutic intervention in the pathway in an animal model of diabetic retinopathy.

* This work was supported by the British Heart Foundation (FS/04/09 and BS/06/005), the Wellcome Trust (79633), a University of West of England Bristol PhD Studentship, the Richard Bright VEGF Research Trust, Fight for Sight, Cancer Research UK (C11392/A10484), and the Skin Cancer Research Fund.

⌘ *Author's Choice*—Final version full access.

[1] Both authors contributed equally to this work.

[2] Joint senior authors.

[3] To whom correspondence may be addressed. E-mail: Michael.Ladomery@uwe.ac.uk.

[4] To whom correspondence may be addressed. E-mail: Dave.Bates@bris.ac.uk.

[5] The abbreviations used are: VEGF, vascular endothelial growth factor; IGF-1, insulin-like growth factor; nt, nucleotide; PBS, phosphate-buffered saline; PKC, protein kinase C; ELISA, enzyme-linked immunosorbent assay; MBP, maltose-binding protein; PSS, proximal splice site selection; OIR, oxygen-induced retinopathy; UTR, untranslated region; ITS, insulin transferrin selenium; PMA, phorbol myristate acetate; HEK, human embryonic kidney.

TABLE 1
Primer sequences

Construct A	Forward:5′-GAATTCCTCATCGCCAGGCCTCCTCACTTG-3′
	Reverse:5′-GGATTCCCTTCGCCGGAGTCTCGCCCTC-3′
Construct B	Forward:5′-GAATTCCGCCCTAACCCCAGCCTTTGTTTTCCATTTCCC-3′
	Reverse:5′-GGATCCGGACTGTTCTGTCGATGGTG-3′
Construct C	Forward:5′-GAATTCCGCCCTAACCCCAGCCTTTGTTTTCCATTTCCC-3′
	Reverse:5′-GGATCCTGGTTCCCGAAACCCTGAGCG-3′
Construct D	Forward:5′-GATTCCGAGGAAGGAAGGAGCCTCCCTCAGGG-3′
	Reverse:5′-GGATCCGGACTGTTCTGTCGATGGTG-3′
Construct E	Forward:5′-GAATTCATGTGACAAGCCGAGGCGG-3′
	Reverse:5′-GGATCCCTGGTTCCCGAAACCCTGAGCG-3′
Mouse VEGF-A ex 7 F	Forward 5′ GTTCAGAGCGGAGAAAGCAT-3′
Mouse VEGF-A ex 8a R	Reverse 5′TCACATCTGCAAGTACGTTCG-3′
Mouse VEGF-A ex 2 F	Forward 5′ AAGGAGAGCAGAAGTCCCATGA-3′
Mouse VEGF-A ex 3 R	Reverse 5′ CTCAATCGGACGGCAGTAGCT-3′
β-Actin F	Forward 5′ AGCCATGTACGTAGCCATCC-3′
β-Actin R	Reverse 5′ CTCTCAGCTGTGGTGGTGAA-3′

EXPERIMENTAL PROCEDURES

Proliferating Podocytes—PCIPs (courtesy of Moin Saleem, University of Bristol, Bristol, UK) were derived from a cell line conditionally transformed from normal human podocytes with a temperature-sensitive mutant of immortalized SV-40 T-antigen. At the permissive temperature of 33 °C, the SV-40 T-antigen is active and allows the cells to proliferate rapidly (16). PCIPs were cultured in T75 flasks (Greiner) in RPMI 1640 medium (Sigma) with 10% fetal bovine serum, 1% ITS (insulin transferrin selenium) (Sigma), 0.5% penicillin-streptomycin solution (Sigma), and grown to 95% confluency. Then cells were split into 6-well plates (2×10^5 cells per well) and grown until 95% confluency.

Treatments with IGF-1 and Pharmacological Inhibitors—To investigate the inhibitory effect of IGF-1 on $VEGF_{xxx}b$ mRNA and protein synthesis, pharmacological inhibitors and IGF-1 with PKC-BIMI (Calbiochem), and SRPK1/2 (SR protein kinases 1 and 2)-SRPIN340 (SR protein phosphorylation inhibitor 340) (17) were used. 24 h before treatment, cultured medium was replaced with serum-free RPMI 1640 medium (Sigma) containing 1% ITS (Sigma) and 0.5% penicillin-streptomycin (Sigma). Subsequently, the medium was replaced with fresh serum-free RPMI 1640 medium (Sigma) containing 1% ITS, 0.5% penicillin-streptomycin, and either 2.5 μM BIMI (bisindolylmaleimide 1) or 10 μM SRPIN340 for 60 min before treatment with IGF-1. 12 h after stimulation, RNA was extracted, and 48 h after stimulation, proteins were extracted.

RT-PCR—1 μg of mRNA was reverse transcribed using MMLV RT, RNase H Minus, point mutant (Promega), and $oligo(dT)_{15}$ (Promega) as a primer. The reaction was carried out in Bio-Rad cycler for 60 min at 40 °C, and then the enzyme was inactivated at 70 °C for 15 min. Ten percent of the cDNA was then amplified using primers designed to pick up proximal and distal splice forms. 1 μM of each primer (exon 7b 5′-GGCAGCTTGAGTTAAACGAAC-3′, exon 8b 5′-ATGGATCCGTATCAGTCTTTCCTGG-3′) and PCR Master Mix (Promega) were used in reactions cycled 30 times, denaturing at 95 °C for 60 s, annealing at 55 °C for 60 s, and extending at 72 °C for 60 s. PCR products were run on 2.5% agarose gels containing 0.5 μg/ml ethidium bromide and visualized under a UV transilluminator. This reaction usually resulted in one amplicon of 130 bp ($VEGF_{xxx}$) and one amplicon of 64 bp ($VEGF_{xxx}b$). For HEK293 and HeLa cells, RT-PCR was performed using primers specific to exon 7a and the 3′-untranslated region of the VEGF mRNA. The primers used were 5′-GTAAGCTTGTACAAGATCCGCAGACG-3′ and 5′-ATGGATCCGTATCAGTCTTTCCTGG-3′. The reaction was set up in a 20-μl reaction using the 2× FastStart Universal SyBR Master Mix (Roche, cat. no: 04913850001) and 1 μM each primer. The reaction was performed on the ABI 7000 cycler for 95 °C for 10 min, followed by 30 cycles of 95 °C for 15 s and 55 °C for 30 s.

Western Blotting—Protein samples were dissolved in Laemmli buffer, boiled for 3–4 min, and centrifuged for 2 min at 20,000 × *g* to remove insoluble materials. 30 μg of protein per lane were separated by SDS/PAGE (12%) and transferred to a 0.2-μm nitrocellulose membrane. The blocked membranes were probed overnight (4 °C) with antibodies against panVEGF (R&D; MAB 293, 1:500), $VEGF_{xxx}b$ (R&D Systems; MAB3045; 1:250), ASF/SF2 antibody (Santa Cruz Biotechnology; sc-10254; 1:1000), and β-tubulin (Sigma, 1:2000). Western blotting has previously shown that all the proteins recognized by the $VEGF_{xxx}b$ antibody are also recognized by commercial antibodies raised against $VEGF_{165}$. It binds recombinant $VEGF_{165}b$, and can be used to demonstrate expression of $VEGF_{165}b$, $VEGF_{189}b$, and $VEGF_{121}b$ (collectively termed $VEGF_{xxx}b$) but does not recognize $VEGF_{165}$, conclusively demonstrating that this antibody is specific for $VEGF_{xxx}b$ (6). Subsequently, the membranes were incubated with secondary horseradish peroxidase-conjugated antibody, and immunoreactive bands were visualized using ECL reagent (Pierce). Immunoreactive bands corresponding to panVEGF and $VEGF_{xxx}b$ in each treatment were quantified by ImageJ analysis and normalized to those of β-tubulin or β-actin. Blots are representative of at least three experiments. Densitometry was carried out by scanning in gels and using ImageJ to determine gray levels of bands and background.

Construction of Plasmids—The VEGF sequence of interest (from 35-bp upstream of exon 8a to 35-bp downstream of exon 8b) was amplified from a BAC DNA template using 50 ng of BAC DNA, 10 μM of each primers (see Table 1), 10 mM dNTP mix (Promega), and Taq polymerase (Promega). A modified ADML-MS2 plasmid was digested with EcoR1 and BamH1, and PCR products ligated into the vector and subsequently transformed. Colonies were selected, and plasmid extraction (Qiagen) was performed. The identities of the plasmids were confirmed by sequencing.

Expression of the MS2-MBP (Maltose-binding Protein) Fusion Protein—MS2-MBP (a gift from Robin Reed, Harvard University) was expressed in *Escherichia coli* DH5α. The cells were grown to an optical density of ~0.5 at 600 nm and induced for expression for 3 h with 0.2 mM isopropyl-1-thio-β-D-galactopyranoside. The MS2-MBP protein was purified by amylose beads according to the manufacturer's protocol (NEB, Beverly, MA). The protein was dialyzed with 10 mM sodium phosphate, pH 7, overnight at 4 °C, to remove existing salts that are present and further purified over a Heparin Hi Trap column using a NaCl gradient (GE Healthcare). An immunoblot analysis was performed on the purified fusion proteins using rabbit anti-MS2 antibody (gift from Peter Stockley, Leeds University) to confirm the identity of the protein.

Assembly of the MS2-MBP System—1 μg of the VEGF-MS2 plasmid was linearized with XbaI and in *vitro* transcribed with T7 RNA polymerase (NEB) in 0.5 mM rNTP (Ambion), 40 mM Tris-HCl, 6 mM $MgCl_2$, 10 mM dithiothreitol, 2 mM spermidine at 40 °C for 1 h to make VEGF-MS2 RNA. A 100-fold molar excess of MS2-MBP fusion protein and VEGF-MS2 RNA were incubated in a buffer containing 20 mM HEPES, pH 7.9 and 60 mM NaCl on ice for 30 min. 75 mg of HEK293 nuclear extract were added to the MS2-MBP fusion protein/VEGF-RNA mix in 0.5 mM ATP, 6.4 mM $MgCl_2$, 20 mM creatine phosphate for 1 h at 30 °C. Proteins that bound to the MS2-MBP/VEGF-MS2 RNA complex were affinity selected on amylose beads by rotating for 4 h at 4 °C and eluted with 12 mM maltose, 20 mM HEPES pH 7.9, 60 mM NaCl, 10 mM β-mercaptoethanol, and 1 mM phenylmethylsulfonyl fluoride.

RNA Immunoprecipitation—HEK293 cells were transfected with plasmid containing the last 131 nt of intron 7 and the first 152 nt of exon 8 inserted downstream of the CMV promoter in pTARGET. Two variants of this were generated by site-directed mutagenesis: a deletion of 11 nucleotides upstream of the PSS from −4 to −24 nt, and the second is a mutation of the sequence CTTTGTTTTCCATTTC to GGGGGGGGGGCAGGGG. Cells were cross-linked for 10 min at 4 °C with 1% formaldehyde in phosphate-buffered saline and blocked by the addition of glycine, pH 8, at a final concentration of 250 mM. The cells were washed twice with PBS, and the cell pellet resuspended in 500 μl of radioimmune precipitation assay buffer (50 mM, Tris-Cl, pH 7.5, 150 mM NaCl, 1 mM EDTA, 1% Nonidet P-40, 0.5% sodium deoxycholate, 0.05% SDS) and incubated on ice for 20 min. The cells were sonicated three times for 15 s with an XL ultrasonic homogenizer (setting 5) and incubated on ice for 2 min between each sonication. The extract was centrifuged for 10 min at 10,000 rpm and precleared by a 1-h incubation at room temperature with protein A-agarose beads (previously coated with 0.5 mg/ml bovine serum albumin and 0.2 mg/ml herring sperm DNA). The antibodies mouse IgG (vector I-200) or anti-ASF/SF2 (SC96, Santa Cruz Biotechnology) were incubated for 1 h at room temperature with protein A-agarose beads (Sigma, coated as above). ASF/SF2-containing complexes were pulled down after a 2-h incubation of the precleared extract with the antibody/beads and washed six times for 10 min each in 50 mM Tris-Cl, pH 7.5, 1 M NaCl, 1 mM EDTA, 1% Nonidet P-40, 1% sodium deoxycholate, 0.1% SDS, 1.5 M urea. The complexes were eluted and cross-link reversed by treatment for 45 min at 70 °C with 50 mM Tris-Cl, pH 7.5, 5 mM EDTA, 10 mM dithiothreitol, and 1% SDS. RNA was then extracted with Tri-reagent solution (Ambion) according to the manufacturer's protocol, precipitated with 0.8 volumes of isopropyl alcohol in the presence of glycoblue (Ambion), the pellet resuspended in water, and subjected to DNase treatment for 1 h at 37 °C and reverse transcription for 1 h at 42 °C using MMLV (Promega) and oligo$(dT)_{15}$. PCR was carried out using the Master Mix from Promega and specific primers for the plasmid VEGF sequence. 5′-CTAGCCTCGAGACGCGTGAT-3′ and 5′-GGCAGCGTGGTTTCTGTATC-3′ or GAPDH.

Oxygen-induced Retinopathy (OIR)—The OIR model was performed as previously described (18, 19) with minor modifications. Neonatal C57/Bl6 mice and nursing CD1 dams were exposed to 75% oxygen between P7 and P12. Return to room air induced hypoxia in the ischemic areas. On P13, mice received either HBSS or SRPIN340 (10 pmol) in Hank's-buffered solution in a 1-μl intraocular injections using a Nanofil syringe fitted with a 35-gauge needle (WPI, Sarasota, FL) into the left eye under isoflurane anesthesia. On P17, both eyes were dissected, fixed in 4% paraformaldehyde overnight at 4 °C, and retinas were dissected. Retinas were permeabilized in PBS containing 0.5% Triton X-100 and 1% bovine serum albumin, stained with 20 μg/ml biotinylated isolectin B4 (Sigma Aldrich) in PBS, pH 6.8, 1% Triton X-100, 0.1 mM $CaCl_2$, 0.1 mM $MgCl_2$, followed by 20 μg/ml ALEXA 488-streptavidin (Molecular Probes, Eugene, OR) and flat mounted in Vectashield (Vector Laboratories, Burlingame, CA). Retinas were examined under a Nikon Eclipse 400 epifluorescence microscope and areas of neovascularization identified under a 4× objective. Images were captured and imported into Image J, and neovascular, ischemic, and normal areas were traced and measured. Imaging was done by investigator, blinded to treatment.

Real-time PCR on Mouse OIR Retina—HBSS or 100 pmol of SRPIN340 in 1 μl was injected intraocularly into OIR pups on day 13 (day 7–12 in 75% O_2), and after 48 h, the eyes were enucleated and placed in RNAlater (Sigma Aldrich), and the retinae were excised. Total RNA was extracted using RNAeasy (Qiagen) according to the manufacturer's manual, and 0.3 μg of DNase-digested total RNA was reverse transcribed using the oligo(dT_{15}) primer. Real-time PCR was performed on a Cepheid Real time thermocycler using ABsolute QPCR SYBR green mix (Thermo Scientific) and 70 nM primers specific for $VEGF_{165}$ (exon 7/8a) or total VEGF (exon 2/3) at 95 °C for 15 min, then 95 °C for 15 s, and 60 °C for 30 s × 40 cycles or for the housekeeping gene (β-actin) 95 °C 15 min, at 95 °C for 15 s, 55 °C for 30 s, 72 °C for 30 s × 40 cycles.

Immunocytofluorescence—Cells were washed with PBS, fixed for 5 min with 4% (w/v) PFA, washed with PBS in 0.05% Triton X (PBS-T) blocked in 5% horse serum in PBS-T (1 h), washed three times, and incubated overnight with 2 μg/ml of anti-ASF/SF2 (SC10255) or a nonspecific goat IgG, washed, and incubated with donkey anti-goat Alexa Fluor 594 for visualization and counterstained for the nucleus with Hoechst. Images were taken at 40× magnification with the Nikon Eclipse 400 epifluorescence microscope or 60× on a Perkin Elmer Ultraview-Fret H confocal microscopy system.

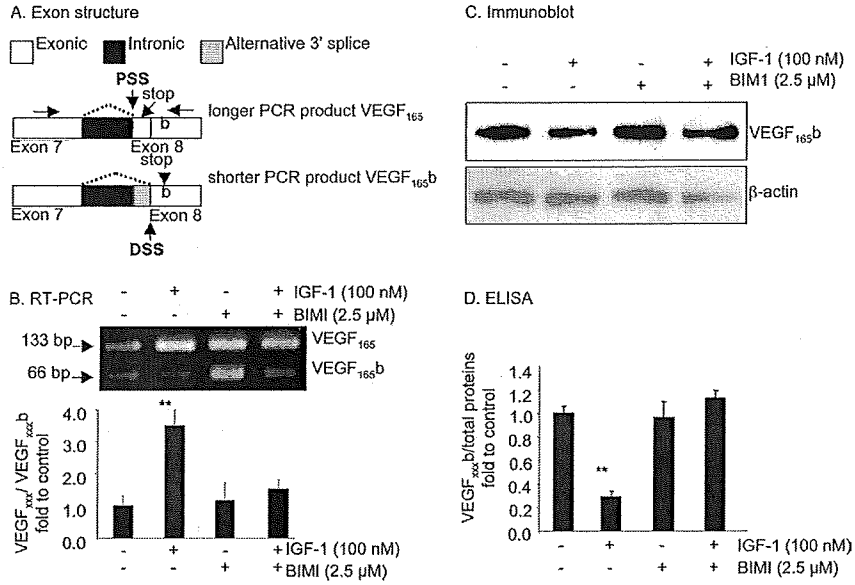

FIGURE 1. **Inhibition of PKC by BIM1 prevents the down-regulation of $VEGF_{xxx}b$ by IGF.** *A*, exon structure of the VEGF pre-mRNA. Alternative splicing of exon 8 to either 8a or 8b results in use of proximal (*PSS*) or distal splice sites (*DSS*) resulting in shorter mRNA for distal splicing. Because the last stop codon is missing, the final six amino acid open reading frame is replaced by an identically sized open reading frame encoding six different amino acids. The primer position is shown by *horizontal arrows*. *B–D*, podocytes were treated with BIM1 (2.5 μM) alone or in combination with IGF-1 (100 nM). *B*, RT-PCR showed that BIM1 reduced the $VEGF_{xxx}$:$VEGF_{xxx}b$ ratio at the RNA level. *C*, Western blot demonstrating that BIM1 inhibited the IGF-mediated down-regulation of $VEGF_{xxx}b$ expression at the protein level. *D*, ELISA results confirming that BIM1 specifically attenuated the IGF-1-dependent down-regulation of $VEGF_{xxx}b$, but does not affect endogenous expression of $VEGF_{xxx}b$. **, $p < 0.01$ compared with untreated.

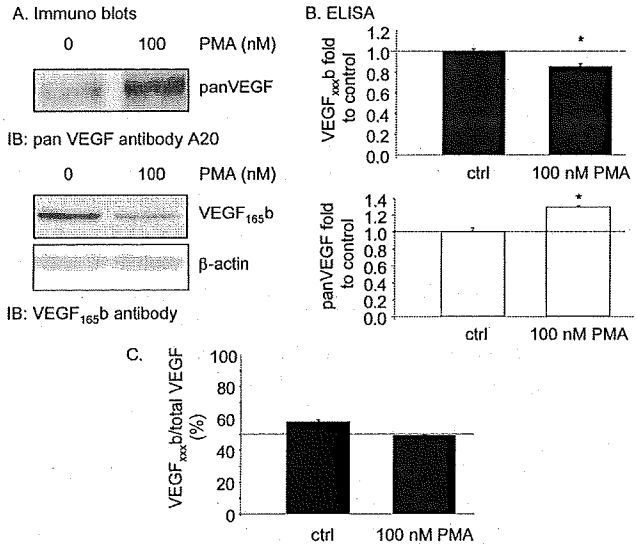

FIGURE 2. **Proximal splicing is activated by protein kinase C.** *A–C*, treatment of podocytes with the PKC activator PMA reduced $VEGF_{165}b$ expression, but increased expression of total VEGF as measured by Western blot (*A*) and ELISA (*B*). This results in a change of relative expression from 60% (anti-angiogenic) to just under 50% (angiogenic) (*C*).

Statistical Analysis—Statistical analyses were carried out on raw data using the Friedman test (Dunnet post-test), and a p value of less than 0.05 was considered statistically significant. Values are expressed as means ± S.E. For all data, n represents the number of independent cell populations or derived from different donors.

RESULTS

The IGF-1-dependent Switch between Isoforms Is PKC-dependent—To determine whether the IGF-1-mediated switch in splicing was regulated by PKC inhibition, podocytes were incubated with pharmacological inhibitors of PKC (BIMI). Treatment with 100 nM IGF-1 and 2.5 μM BIMI, the PKC inhibitor, followed by RNA extraction and RT-PCR using primers that detect both proximal ($VEGF_{xxx}$, 130-bp amplicon) and distal splice isoforms ($VEGF_{xxx}b$, 64 bp amplicon) was carried out. Treatment with IGF-1 increased the relative intensity of the $VEGF_{xxx}$ (upper) band to the $VEGF_{xxx}b$ band (lower) from 1.39 ± 0.42 to 4.84 ± 0.65 ($p < 0.01$, Fig. 1*B*). Treatment with 100 nM IGF-1 and 2.5 μM BIMI, the PKC inhibitor, resulted in a $VEGF_{xxx}$:$VEGF_{xxx}b$ density of 2.12 ± 0.39, which was lower than treatment with IGF-1 alone (4.84 ± 0.65, $p < 0.05$) but was not different from treatment with BIMI alone (1.62 ± 0.76, $p > 0.05$, Fig. 1*B*).

To determine whether IGF-1-mediated regulation of splicing was apparent at the protein level, podocytes were incubated with the pharmacological inhibitors of PKC (BIMI), and ELISA carried out on the protein extracted from the cells. Treatment with 100 nM IGF-1 and 2.5 μM BIMI, the PKC inhibitor, resulted in cells producing 0.47 ± 0.03 pg/μg of $VEGF_{xxx}b$, which was significantly greater than cells treated with IGF-1 alone (0.12 ± 0.02 pg/μg, $p < 0.001$) but was not different from treatment with BIMI alone (0.40 ± 0.06 pg/μg, $p > 0.05$, Fig. 1*D*). This was confirmed by Western blot (Fig. 1*C*).

PKC Activation Induces Proximal Splice Site Selection—To determine whether the PKC activation was sufficient to cause proximal splice site selection, cells were treated with 100 nM phorbol myristate acetate (PMA), which is known to induce PKC activation. PMA treatment resulted in a significant increase in VEGF expression as determined by Western blot, but a decrease in $VEGF_{165}b$ expression (Fig. 2*A*). To confirm this quantitatively, ELISA was performed on protein extracted from these cells, and a significant reduction in $VEGF_{165}b$ but increase in total VEGF was seen (Fig. 2*B*). This results in a decrease in the relative $VEGF_{xxx}b$ levels (Fig. 2*C*).

SRPK1/2 Inhibition Prevents the Down-regulation of $VEGF_{xxx}b$ by IGF-1—There are a number of splicing factor kinases that are activated by PKC, including the SR protein kinases SRPK1 and SRPK2 (20, 21). To test the effect of SRPIN340, an inhibitor of SRPK1/2, on IGF-1-mediated down-regulation of $VEGF_{xxx}b$ at the protein and mRNA level, cells were treated with SRPIN340 (10 μM) alone and then in combi-

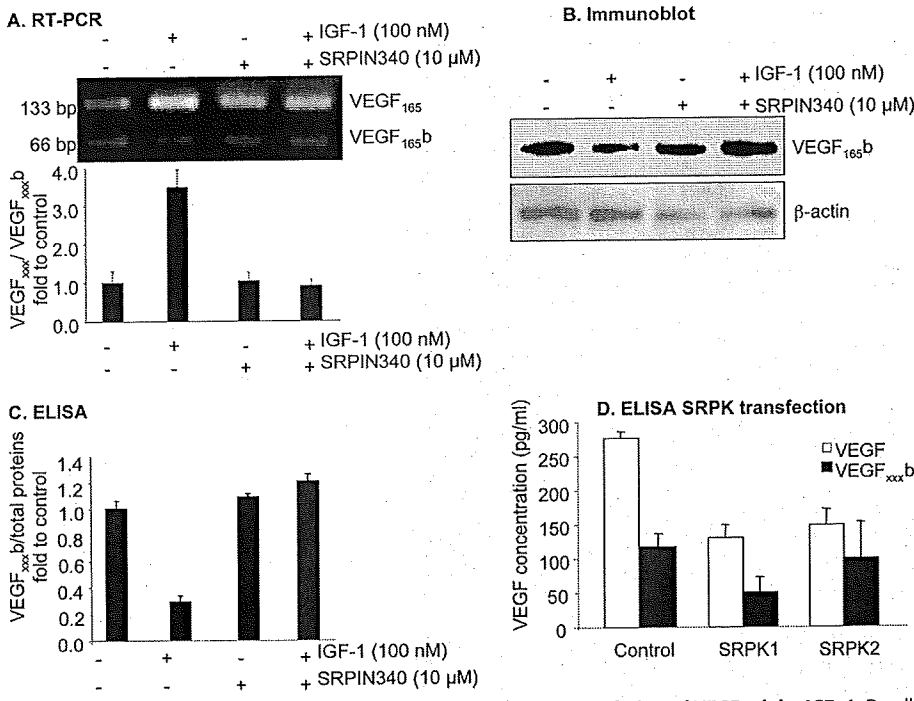

FIGURE 3. **Inhibition of SPRK1/2 by SRPIN340 prevents the down-regulation of $VEGF_{xxx}b$ by IGF.** *A–D*, cells were treated with SRPIN340 (10 μM) alone or in combination with IGF-1 (100 nM). *A*, RT-PCR showed that SRPIN340 reduced the $VEGF_{165}$:$VEGF_{165}b$ ratio at the RNA level. *B*, Western blot demonstrating that SRPIN340 inhibited the IGF-mediated down-regulation of $VEGF_{xxx}b$ expression at the protein level. *C*, ELISA results confirming that SPRIN340 specifically attenuates the IGF-1-dependent down-regulation of $VEGF_{xxx}b$, but did not affect endogenous expression of $VEGF_{xxx}b$. *D*, ELISA of the protein extract shows that SRPK1 transfection reduces $VEGF_{xxx}b$ expression, and total VEGF expression. SRPK2 reduces total expression, but did not affect $VEGF_{xxx}b$ expression.

nation with IGF-1 (100 nM). Amplification of cDNA from podocytes showed that IGF-1 treatment with 10 μM SRPIN340, the SRPK1/2 inhibitor resulted in a relative $VEGF_{xxx}$:$VEGF_{xxx}b$ density of 1.26 ± 0.22, which was lower than treatment with IGF-1 alone (4.84 ± 0.65, $p < 0.01$) but was not different from treatment with SRPIN340 alone (1.45 ± 0.30, $p > 0.05$, Fig. 3*A*). At the protein level, SRPIN340 inhibited IGF-1-dependent down-regulation of $VEGF_{xxx}b$ from 0.12 ± 0.02 pg/μg to 0.50 ± 0.05 pg/μg ($p < 0.001$), but not when SRPIN340 was used alone (0.45 ± 0.01 pg/μg), indicating that SRPK inhibition did not affect endogenous expression of $VEGF_{xxx}b$ (0.42 ± 0.02 pg/μg, $p > 0.05$) (Fig. 3*C*). This was again confirmed by Western blot (Fig. 3*B*). To confirm the involvement of SRPK1 or SRPK2 in the terminal splice site choice, epithelial cells were transfected with expression vectors to overexpress SRPK1 and SRPK2. Fig. 3*D* shows that overexpression of SRPK1, but not SRPK2, resulted in reduced distal splice site selection and hence reduced overall VEGF levels. By itself, it was not sufficient to simply switch the splicing but resulted in inhibition of $VEGF_{165}b$ without increased $VEGF_{165}$. Interestingly, SRPK2 overexpression did not affect $VEGF_{165}b$ production, although it did reduce total VEGF expression.

IGF1 Treatment Resulted in Nuclear Localization of ASF/SF2, which Was Blocked by SPRK1/2 Inhibition—SRPK1 has been shown to phosphorylate ASF/SF2, which we have previously shown to favor proximal splice site selection. To determine whether IGF-1 altered ASF/SF2 localization, podocytes were treated with 100 nM IGF and stained for ASF/SF2. Untreated cells (Fig. 4*A*) contained both nuclear and cytoplasmic ASF/SF2, whereas after treatment with IGF-1, ASF/SF2 localized specifically to the nucleus (Fig. 4*B*). This localization was inhibited by SRPIN340 (Fig. 4, *B versus D*), indicating that IGF1-mediated activation of SRPK1/2 was responsible for the nuclear localization of ASF/SF2. It has previously been demonstrated that ASF/SF2 can be shuttled from the nucleus to the cytoplasm in HeLa cells, but is predominantly nuclear. We therefore investigated ASF/SF2 localization in these and another cell type, HEK293 cells. Fig. 4, *E* and *F* shows that whereas in HEK293 cells there is a strong cytoplasmic localization for the ASF/SF2, in HeLa cells expression is predominantly nuclear, as previously described. This subcellular localization of ASF/SF2 was confirmed by the use of a second ASF/SF2 antibody. Furthermore, high resolution gel electrophoresis showed that whereas podocyte cytoplasmic protein contains a single molecular weight ASF/SF2, an additional higher molecular weight band is seen in podocyte nuclei (data not shown), confirming that in podocytes ASF/SF2 is both cytoplasmic and nuclear. We also investigated $VEGF_{165}b$ mRNA expression in these two additional cell types. Fig. 4*G* shows that HEK cells (with cytoplasmic ASF/SF2) express $VEGF_{165}b$, whereas HeLa cells (nuclear ASF/SF2) only express $VEGF_{165}$. This is consistent with the cytoplasmic location of ASF/SF2 being associated with $VEGF_{165}b$ expression.

ASF/SF2 Requires a 35-nt Region around the Proximal Splice Site of Exon 8 to Bind to VEGF mRNA—To determine whether ASF/SF2 could bind directly to the proximal splice site RNA, we used the MS2-MBP system to pull-down proteins that could interact with the RNA. Fig. 5*A* shows that ASF/SF2 was present both in crude nuclear extract and in the pull-down of nuclear extract incubated with an RNA containing the MS2 binding domain RNA fused to an 88-nt fragment containing the initial 35 nucleotides upstream of exon 8a, the coding sequence of exon 8a, and 35 nucleotides of 3′-UTR. In contrast, less ASF/SF2 was seen in the pull-down of nuclear extract incubated with the mRNA that did not have the 35 nucleotides upstream of exon 8a and did not bind the MS2 binding domain by itself, indicating that ASF/SF2 required a 35-nt fragment of exon 8a upstream of the proximal splice site to most efficiently bind the VEGF pre-mRNA. To determine whether binding of ASF/SF2 was PKC-dependent and whether this was SRPK1-dependent, HEK293 cells were treated with the PKC activator PMA in the presence or absence of the SRPK inhibitor SRPIN340, and then the protein run on an MS2-MBP column

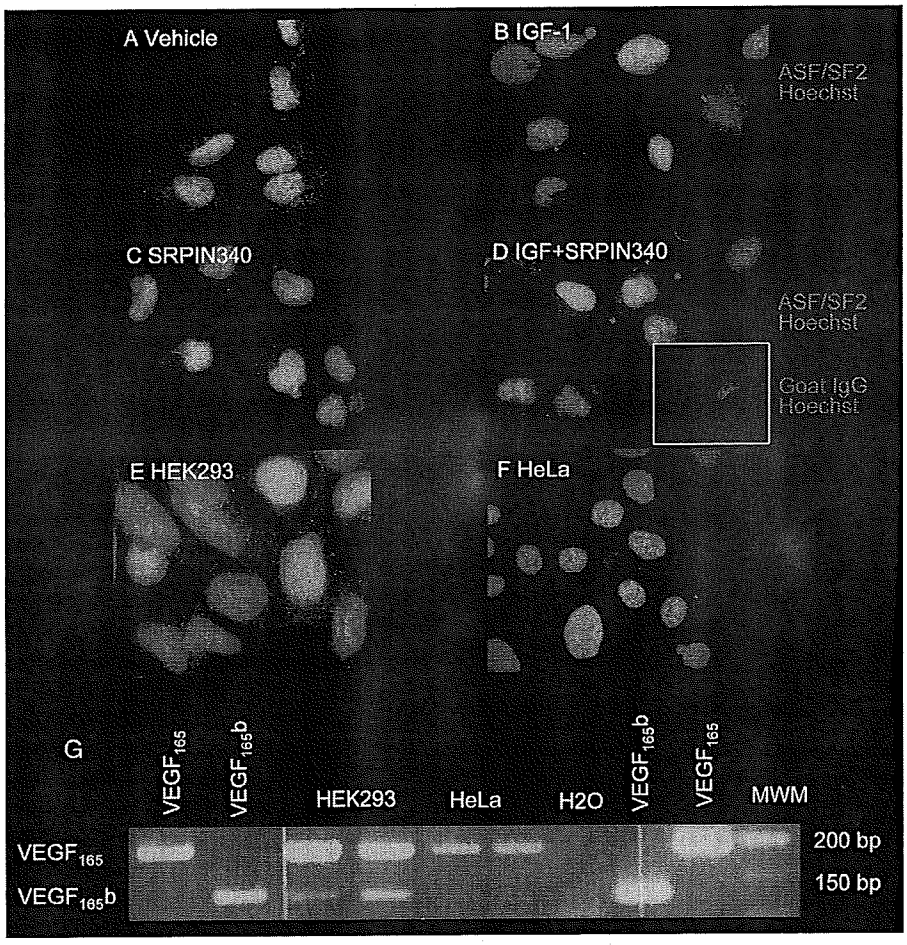

FIGURE 4. **Nuclear localization of ASF/SF2 is increased by IGF-1.** *A–F*, cells were treated with vehicle or IGF in the presence or absence of SRPIN340 and stained for ASF/SF2 and counterstained with Hoechst. *A*, podocytes show expression of ASF/SF2 in the nucleus and in the cytoplasm. *B*, IGF induces nuclear localization of cytoplasmic ASF/SF2. *C*, SRPIN340 by itself does not affect localization of ASF/SF2. *D*, SRPIN340 inhibited this IGF-mediated localization. *E*, HEK cells also show cytoplasmic localization of ASF/SF2. *F*, in contrast, HeLa cells have nuclear ASF/SF2 localization. *G*, RT-PCR of mRNA from HEK cells shows $VEGF_{165}b$ expression, but not in HeLa cells. *MWM*, molecular weight marker.

with the VEGF exon 8 construct. Fig. 5*B* shows that in cells treated with PMA, more ASF/SF2 binds to the VEGF construct than in untreated cells. This increase was inhibited by treatment with 10 μM SRPIN340 or by treatment with the phosphatase PP1. The sequence 35 nucleotides upstream of the PSS contains ASF/SF2 and U2AF65 consensus binding sequences. To determine more precisely the sequence required for ASF/SF2 binding to the RNA, a short sequence upstream of the proximal splice site was mutated (14 nt) or deleted (11 nt) in a plasmid containing just the terminal part of intron 7 and the proximal part of exon 8. Fig. 5*D* shows that the three constructs express the recombinant VEGF RNA (total cell extract, TCE). However, only the wild-type RNA was pulled-down with the ASF/SF2 protein, suggesting that the region we have mutated or deleted is required for ASF/SF2 binding to the VEGF pre-mRNA.

SRPK1/2 Inhibition Inhibits Angiogenesis in a Mouse Model of Retinal Neovascularization—To determine whether the inhibition of proximal splice site selection by blocking SRPK1/2, and hence increased anti-angiogenic $VEGF_{165}b$ production, we used a mouse model of retinal neovascularization where angiogenesis is driven by hypoxia, a process known to favor proximal splice site selection. Injection of SRPIN340 into mouse retina resulted in a significant inhibition of neovascular area of the retina, as well as a significant reduction in ischemic area (Fig. 6, *C*, *D*, and *F*). This resulted in a significant increase in the normally vascularized area, a result that is qualitatively consistent with injection of recombinant $VEGF_{165}b$ into the vitreous in this model (Fig. 6, *E* and *F*). To determine whether VEGF levels were altered by SRPIN340 treatment, mRNA was extracted from the retinae and subjected to Q-PCR for all VEGF isoforms using primers in exon 2 and 3. Treatment of eyes with SRPIN340 made no difference in overall VEGF levels (2.3 ± 0.5% of actin compared with 2.2 ± 2.0%). However, exon 8a containing mRNA was altered from 1.1 ± 0.5 to 0.3 ± 0.2% of actin).

DISCUSSION

VEGF induction by IGF-1 occurs via different signaling pathways including PKC (22) and PI3-K (23–25). There is increasing evidence that transducing components that link the cell surface with the nuclear splicing machinery implicate signaling pathways such as PKC (26), PI3-K (27, 28), or PKB/Akt (29, 30). IGF-1 modulates splicing of VEGF isoforms by preferential use of the PSS to increase expression of pro-angiogenic isoforms (15). Moreover, previously we have shown that ASF/SF2 overexpression preferentially increases usage of the proximal splice site (15) and gives the same effect as IGF-1. SRPK1 has been shown specifically to phosphorylate 12 serines of the RS domain in ASF/SF2 (31), and SRPK2 has been involved in the localization of ASF/SF2 within the nucleus. Thus, in this report, we have investigated the link between the splicing machinery and IGF-1 signaling.

We have shown that the IGF-1-mediated increase in VEGF isoforms using the proximal splice site is inhibited by blocking PKC and SRPK1/2, and that this can be overcome by the use of a PKC inhibitor or mimicked by a PKC agonist or overexpression of SRPK1. This firmly suggests that this kinase cascade is involved in splice site selection in the *VEGF* gene. We have used RT-PCR, ELISA, and Western blotting to investigate VEGF splicing. VEGF isoform mRNA expression depends on transcription, splicing, and degradation of mRNA, and protein expression additionally depends upon translational rate and degradation rate. The finding that the mRNA and protein iso-

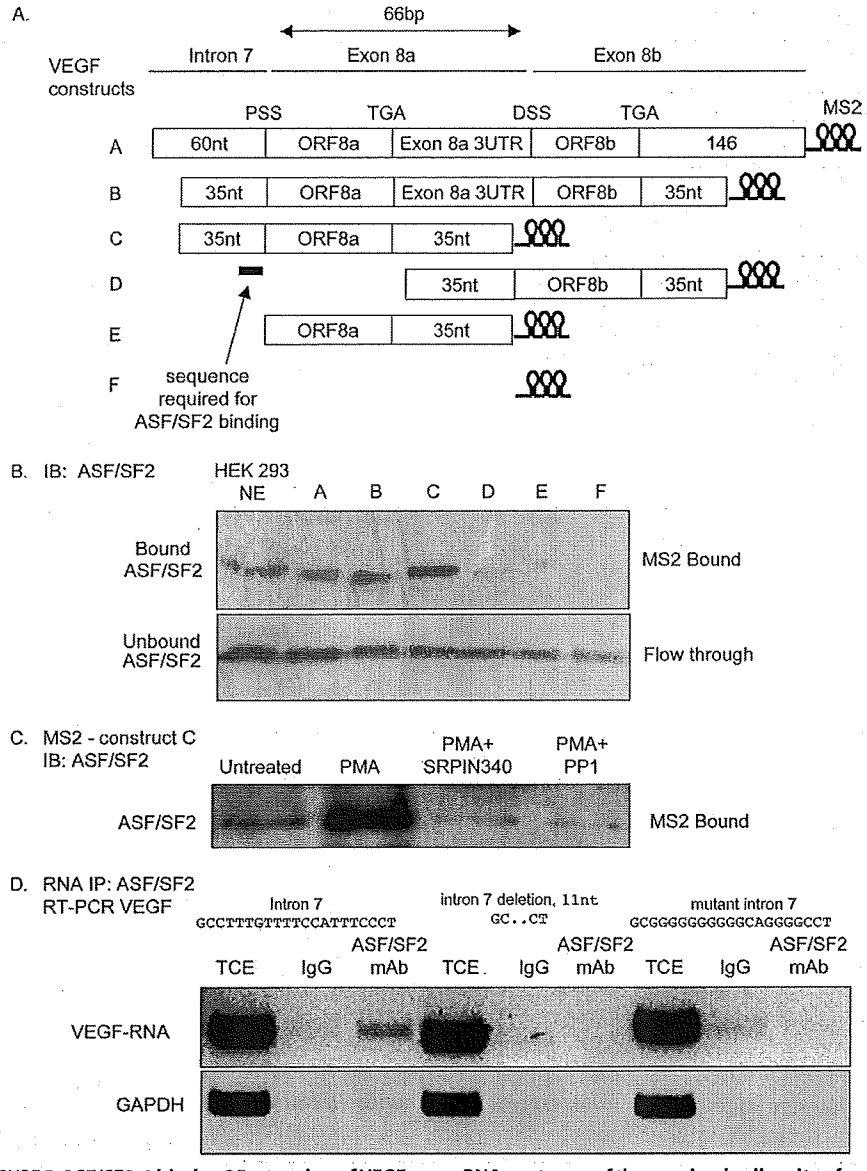

FIGURE 5. **ASF/SF2-1 binds a 35-nt region of VEGF pre-mRNA upstream of the proximal splice site of exon 8.** *A*, constructs were generated containing fragments of the exon 7/exon 8 boundary, fused to a sequence encoding the stem loop structures recognized by the MBP-MS2-binding protein, which can bind maltose. These were transcribed *in vitro*. *B*, Western blot of HEK cell crude nuclear extract (*NE*) or NE incubated with mRNA constructs as above and run over a maltose column to isolate proteins that bind to the RNA constructs and probed with an ASF/SF2 antibody. Whereas mRNA containing the 5′ regions of the intron 7/exon 8 boundary contained ASF/SF2 immunoreactivity, RNA encoding the exon 8 region did not, identifying the binding site for ASF/SF2 in the intron 7/exon 8a boundary. *C*, immunoblot of HEK cell NE of cells treated as shown incubated with the RNA construct C and run over the MS2-MBP column. PMA activation increased binding, and this was blocked by SRPIN340 and phosphatase treatment. *D*, RNA immunoprecipitation of ASF/SF2 in cells expressing constructs with a mutated or deleted intron 7 sequence. The *top* shows RT-PCR of total cell extract (*TCE*) or immunoprecipitated RNA using a nonspecific mouse IgG (*IgG*), or using a mouse monoclonal antibody to ASF/SF2 using primers to detect the VEGF sequence. The *bottom blot* shows the same treatments subjected to GAPDH amplification. The wild-type sequence showed a stronger band in the ASF/SF2 IP, whereas the mutants showed no difference between mouse IgG and ASF/SF2.

forms are both altered in a similar way by each intervention suggests that this is an mRNA switch, at least in part. As the mRNAs are generated by alternative splicing it is unlikely that differential isoform production is due to differential transcription, as both isoforms are transcribed from the same promoter region. However, VEGF has been shown to have two alternate transcription start sites. Although there is no evidence to date to show that these are differentially used for the different exon 8 isoforms, they do confer different exon 7 inclusion (32). If alternate transcription start sites are used, the splicing machinery would still need to be different in order for the transcription complex to recognize the different exon 8 splice sites. It is possible that these two different isoform families are differentially degraded, and that IGF mediates a decrease in degradation of mRNA encoding the proximal splice site. This is a possibility that we have not as yet excluded. However, the finding that ASF/SF2, a known splicing factor, requires the presence of a specific short sequence in the polypyrimidine tract upstream of the proximal splice site and that ASF/SF2 is induced to nuclear localization by SRPK1 activation and IGF-1 activation strongly suggest that this is a splicing mechanism rather than a degradation mechanism. We have shown that ASF/SF2 requires this sequence, which contains both a U2AF65 and consensus ASF/SF2 sequence, for binding to the VEGF pre-mRNA, but does not demonstrate that this is the sequence it binds to. ASF/SF2 binding to a region upstream of a splice site is generally considered a splicing repressor. There is evidence that SR proteins can interact with sequences upstream of the splice site that act as intronic splicing enhancer or silencer regions (reviewed in Ref. 33); for instance in the *FGFR2* gene mutations in 50% of the sequential 6 nucleotide sequences in the intronic region upstream of the splice site resulted in altered splicing (34). However, an alternative explanation is that ASF/SF2 requires the U2AF65 consensus sequence adjacent to exon 8a to be present in order for it to bind to consensus sequences downstream and repress distal splice site selection, and hence when mutated or deleted DSS repression is lifted resulting in preferential proximal splice site selection. More research is required to pinpoint the exact mechanism of splicing regulation by ASF/SF2.

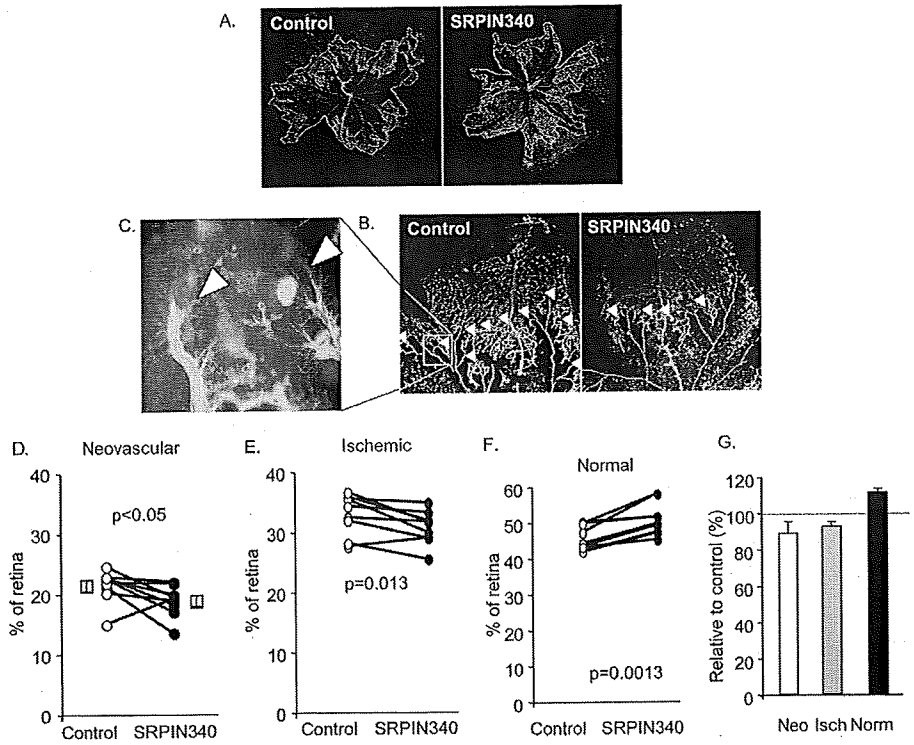

FIGURE 6. **Neovascularization induced by hyperoxia is inhibited by a single dose of SRPK inhibitor, SRPIN340.** *A*, low power fluorescence micrograph of FITC-labeled lectin staining of retinal whole mounts with areas of NV (*white*) and ischemic (*orange*) outlined. *B*, higher power view of a single retinal quadrant, with angiogenic areas highlighted by *arrowheads*. *C*, high power view of retinal angiogenic area showing sprouting endothelial cells. *D*, quantification of neovascular areas shows a small but significant inhibition by a single injection of 1 μl of 10 μM SRPIN340 1 day after removal from oxygen. *E*, ischemic area was also reduced in these mice. *F*, normal area was consequently increased. *G*, data shown as relative to control, uninjected contralateral eye. *Neo*, neovacular; *isch*, ischemia; *Norm*, normal.

It is still not clear if the IGF-1 system plays a direct role in the growth of new blood vessels. However, there are increasing examples that IGF-1 indirectly increases angiogenesis by up-regulation of VEGF (22, 25, 35). Moreover, IGF-1 induces angiogenesis in the rabbit cornea (36) and stimulates migration, proliferation (37), and tube formation of human endothelial cells (38). IGF-1 is also widely implicated in pathological angiogenesis. Expression of IGF-1 was increased in the vitreous of patients with diabetic retinopathy (39). There is a positive correlation between elevated VEGF-A and IGF-1 in different types of cancers such as colorectal cancer (40), breast cancer (41), and head and neck squamous cell carcinomas (25).

Moreover, the *SFRS1* gene, encoding ASF/SF2, fulfills the criteria of a proto-oncogene (42). Overexpression of ASF/SF2 in immortalized rodent fibroblasts resulted in formation of high-grade sarcomas after injection into nude mice (43). Knock-down of ASF/SF2 in lung carcinoma, which has high expression of that molecule, inhibited tumor formation in nude mice (43).

There are increasing examples that manipulation of the splicing machinery can be used as new therapeutic targets (44). Small molecules that can target splicing factors and kinases involved in splicing are promising candidates for drugs (17, 45–47). Alternatively, the use of antisense oligonucleotides such as morpholinos, which can bind to the specific splice sites to modulate aberrant splicing has been investigated (48, 49). SRPK1 seems to be a relatively new target for future cancer therapies but is receiving more attention recently as higher expression of SRPK1 has been observed in breast and colonic tumors, and its increased expression is associated with the grade of a tumor (50). Moreover, it has been shown that known anticancer drugs such as gemcitabine and cisplatin increase cell apoptosis with a much stronger effect when phosphorylation of SR proteins was inhibited by using siRNA against SRPK1 (51). SRPK2 is able to bind and phosphorylate acinus, an SR protein, and moves it from nuclear speckles to the nucleoplasm, resulting in the activation of cyclin A1 (52). Moreover, overexpression of acinus or SRPK2 increased leukemia cell proliferation. SRPK2 and acinus were also overexpressed in human acute myelogenous leukemia patients and correlate with elevated cyclin A1 expression levels (52). These two kinases are able to phosphorylate the splicing factor, ASF/SF2 and all these components are involved in the choice of the PSS in VEGF. The inhibitor of SRPK1/2 kinase, SRPIN340 prevents the down-regulation of the $VEGF_{xxx}b$ isoforms. Moreover, SRPK1 and SRPK2 are known to phosphorylate the ASF/SF2 splicing factor with high specificity (21, 31, 53). These results indicate that an overactivity of SRPK1 can cause phosphorylation of ASF/SF2. However, SRPKs have other targets, including those known to up-regulate $VEGF_{xxx}b$ such as SRp55 (15), and the contribution of SRp55 phosphorylation to IGF-mediated effects (perhaps by inhibiting its binding to the distal splice enhancer region) cannot be ruled out. It thus appears likely that SRPK1-mediated phosphorylation of ASF/SF2 could support an activation of the PSS and increased production of pro-angiogenic isoforms.

The overexpression findings, however, suggest that whereas SRPKs are necessary, they are not sufficient for proximal splice site selection. Thus these findings indicate that SRPK1 inhibitors may be potentially anti-angiogenic, and to that end we set out to investigate this in a model of angiogenesis in the eye. A single dose of SRPIN340 resulted in significant inhibition of angiogenesis and increased normal vascularization. Whereas, we have not measured $VEGF_{165}b$ levels in these eyes, there is a discrepancy between total and exon 8a-containing isoforms that is most likely a result of altered splicing. The angiogenesis is known to be mediated by pro-angiogenic VEGF and can be inhibited by anti-angiogenic $VEGF_{165}b$ (18); thus, allowing us to draw a parallel between anti-angiogenic splice forms and inhibition of splice factors that cause pro-angiogenic splicing in

the same retinal angiogenesis model. These data suggest that anti-SRPK1 inhibitors may be useful anti-angiogenic agents, suggesting a use in cancer as well as diabetic retinopathy or age-related macular degeneration.

REFERENCES

1. Kerbel, R. S. (2008) *N. Engl. J. Med.* **358,** 2039–2049
2. Duh, E., and Aiello, L. P. (1999) *Diabetes* **48,** 1899–1906
3. Slomiany, M. G., and Rosenzweig, S. A. (2004) *Invest. Ophthalmol. Vis. Sci.* **45,** 2838–2847
4. Harper, S. J., and Bates, D. O. (2008) *Nat. Rev. Cancer* **8,** 880–887
5. Houck, K. A., Ferrara, N., Winer, J., Cachianes, G., Li, B., and Leung, D. W. (1991) *Mol. Endocrinol.* **5,** 1806–1814
6. Woolard, J., Wang, W. Y., Bevan, H. S., Qiu, Y., Morbidelli, L., Pritchard-Jones, R. O., Cui, T. G., Sugiono, M., Waine, E., Perrin, R., Foster, R., Digby-Bell, J., Shields, J. D., Whittles, C. E., Mushens, R. E., Gillatt, D. A., Ziche, M., Harper, S. J., and Bates, D. O. (2004) *Cancer Res.* **64,** 7822–7835
7. Bates, D. O., Cui, T. G., Doughty, J. M., Winkler, M., Sugiono, M., Shields, J. D., Peat, D., Gillatt, D., and Harper, S. J. (2002) *Cancer Res.* **62,** 4123–4131
8. Perrin, R. M., Konopatskaya, O., Qiu, Y., Harper, S., Bates, D. O., and Churchill, A. J. (2005) *Diabetologia* **48,** 2422–2427
9. Varey, A. H., Rennel, E. S., Qiu, Y., Bevan, H. S., Perrin, R. M., Raffy, S., Dixon, A. R., Paraskeva, C., Zaccheo, O., Hassan, A. B., Harper, S. J., and Bates, D. O. (2008) *Br. J. Cancer* **98,** 1366–1379
10. Rennel, E., Waine, E., Guan, H., Schüler, Y., Leenders, W., Woolard, J., Sugiono, M., Gillatt, D., Kleinerman, E., Bates, D., and Harper, S. (2008) *Br. J. Cancer* **98,** 1250–1257
11. Pritchard-Jones, R. O., Dunn, D. B., Qiu, Y., Varey, A. H., Orlando, A., Rigby, H., Harper, S. J., and Bates, D. O. (2007) *Br. J. Cancer* **97,** 223–230
12. Schumacher, V. A., Jeruschke, S., Eitner, F., Becker, J. U., Pitschke, G., Ince, Y., Miner, J. H., Leuschner, I., Engers, R., Everding, A. S., Bulla, M., and Royer-Pokora, B. (2007) *J. Am. Soc. Nephrol.* **18,** 719–729
13. Dieudonné, S. C., La Heij, E. C., Diederen, R. M., Kessels, A. G., Liem, A. T., Kijlstra, A., and Hendrikse, F. (2007) *Ophthalmic. Res.* **39,** 148–154
14. Ergorul, C., Ray, A., Huang, W., Darland, D., Luo, Z. K., and Grosskreutz, C. L. (2008) *Mol. Vis.* **14,** 1517–1524
15. Nowak, D. G., Woolard, J., Amin, E. M., Konopatskaya, O., Saleem, M. A., Churchill, A. J., Ladomery, M. R., Harper, S. J., and Bates, D. O. (2008) *J. Cell Sci.* **121,** 3487–3495
16. Saleem, M. A., O'Hare, M. J., Reiser, J., Coward, R. J., Inward, C. D., Farren, T., Xing, C. Y., Ni, L., Mathieson, P. W., and Mundel, P. (2002) *J. Am. Soc. Nephrol.* **13,** 630–638
17. Fukuhara, T., Hosoya, T., Shimizu, S., Sumi, K., Oshiro, T., Yoshinaka, Y., Suzuki, M., Yamamoto, N., Herzenberg, L. A., Herzenberg, L. A., and Hagiwara, M. (2006) *Proc. Natl. Acad. Sci. U.S.A.* **103,** 11329–11333
18. Konopatskaya, O., Churchill, A. J., Harper, S. J., Bates, D. O., and Gardiner, T. A. (2006) *Mol. Vis.* **12,** 626–632
19. Smith, L. E., Wesolowski, E., McLellan, A., Kostyk, S. K., D'Amato, R., Sullivan, R., and D'Amore, P. A. (1994) *Invest. Ophthalmol. Vis. Sci.* **35,** 101–111
20. Gui, J. F., Lane, W. S., and Fu, X. D. (1994) *Nature* **369,** 678–682
21. Wang, H. Y., Lin, W., Dyck, J. A., Yeakley, J. M., Songyang, Z., Cantley, L. C., and Fu, X. D. (1998) *J. Cell Biol.* **140,** 737–750
22. Beckert, S., Farrahi, F., Perveen Ghani, Q., Aslam, R., Scheuenstuhl, H., Coerper, S., Königsrainer, A., Hunt, T. K., and Hussain, M. Z. (2006) *Biochem. Biophys. Res. Commun.* **341,** 67–72
23. Miele, C., Rochford, J. J., Filippa, N., Giorgetti-Peraldi, S., and Van Obberghen, E. (2000) *J. Biol. Chem.* **275,** 21695–21702
24. Poulaki, V., Mitsiades, C. S., McMullan, C., Sykoutri, D., Fanourakis, G., Kotoula, V., Tseleni-Balafouta, S., Koutras, D. A., and Mitsiades, N. (2003) *J. Clin. Endocrinol. Metab.* **88,** 5392–5398
25. Slomiany, M. G., Black, L. A., Kibbey, M. M., Day, T. A., and Rosenzweig, S. A. (2006) *Biochem. Biophys. Res. Commun.* **342,** 851–858
26. Lynch, K. W., and Weiss, A. (2000) *Mol. Cell. Biol.* **20,** 70–80
27. Patel, N. A., Chalfant, C. E., Watson, J. E., Wyatt, J. R., Dean, N. M., Eichler, D. C., and Cooper, D. R. (2001) *J. Biol. Chem.* **276,** 22648–22654
28. Blaustein, M., Pelisch, F., Coso, O. A., Bissell, M. J., Kornblihtt, A. R., and Srebrow, A. (2004) *J. Biol. Chem.* **279,** 21029–21037
29. Blaustein, M., Pelisch, F., Tanos, T., Muñoz, M. J., Wengier, D., Quadrana, L., Sanford, J. R., Muschietti, J. P., Kornblihtt, A. R., Cáceres, J. F., Coso, O. A., and Srebrow, A. (2005) *Nat. Struct. Mol. Biol.* **12,** 1037–1044
30. Patel, N. A., Kaneko, S., Apostolatos, H. S., Bae, S. S., Watson, J. E., Davidowitz, K., Chappell, D. S., Birnbaum, M. J., Cheng, J. Q., and Cooper, D. R. (2005) *J. Biol. Chem.* **280,** 14302–14309
31. Ma, C. T., Velazquez-Dones, A., Hagopian, J. C., Ghosh, G., Fu, X. D., and Adams, J. A. (2008) *J. Mol. Biol.* **376,** 55–68
32. Bastide, A., Karaa, Z., Bornes, S., Hieblot, C., Lacazette, E., Prats, H., and Touriol, C. (2008) *Nucleic Acids Res.* **36,** 2434–2445
33. Voelker, R. B., and Berglund, J. A. (2007) *Genome Res.* **17,** 1023–1033
34. Hovhannisyan, R. H., Warzecha, C. C., and Carstens, R. P. (2006) *Nucleic Acids Res.* **34,** 373–385
35. Wang, Y. Z., and Wong, Y. C. (1998) *Prostate* **35,** 165–177
36. Grant, M. B., Mames, R. N., Fitzgerald, C., Ellis, E. A., Aboufriekha, M., and Guy, J. (1993) *Diabetologia* **36,** 282–291
37. Shigematsu, S., Yamauchi, K., Nakajima, K., Iijima, S., Aizawa, T., and Hashizume, K. (1999) *Endocr. J.* **46,** S59–S62
38. Nakao-Hayashi, J., Ito, H., Kanayasu, T., Morita, I., and Murota, S. (1992) *Atherosclerosis* **92,** 141–149
39. Grant, M., Russell, B., Fitzgerald, C., and Merimee, T. J. (1986) *Diabetes* **35,** 416–420
40. Warren, R. S., Yuan, H., Matli, M. R., Ferrara, N., and Donner, D. B. (1996) *J. Biol. Chem.* **271,** 29483–29488
41. Oh, J. S., Kucab, J. E., Bushel, P. R., Martin, K., Bennett, L., Collins, J., DiAugustine, R. P., Barrett, J. C., Afshari, C. A., and Dunn, S. E. (2002) *Neoplasia* **4,** 204–217
42. Hanahan, D., and Weinberg, R. A. (2000) *Cell* **100,** 57–70
43. Karni, R., de Stanchina, E., Lowe, S. W., Sinha, R., Mu, D., and Krainer, A. R. (2007) *Nat. Struct. Mol. Biol.* **14,** 185–193
44. Hagiwara, M. (2005) *Biochim. Biophys. Acta* **1754,** 324–331
45. Pilch, B., Allemand, E., Facompré, M., Bailly, C., Riou, J. F., Soret, J., and Tazi, J. (2001) *Cancer Res.* **61,** 6876–6884
46. Muraki, M., Ohkawara, B., Hosoya, T., Onogi, H., Koizumi, J., Koizumi, T., Sumi, K., Yomoda, J., Murray, M. V., Kimura, H., Furuichi, K., Shibuya, H., Krainer, A. R., Suzuki, M., and Hagiwara, M. (2004) *J. Biol. Chem.* **279,** 24246–24254
47. Bakkour, N., Lin, Y. L., Maire, S., Ayadi, L., Mahuteau-Betzer, F., Nguyen, C. H., Mettling, C., Portales, P., Grierson, D., Chabot, B., Jeanteur, P., Branlant, C., Corbeau, P., and Tazi, J. (2007) *PLoS Pathog.* **3,** 1530–1539
48. Bruno, I. G., Jin, W., and Cote, G. J. (2004) *Hum. Mol. Genet.* **13,** 2409–2420
49. Wheeler, T. M., Lueck, J. D., Swanson, M. S., Dirksen, R. T., and Thornton, C. A. (2007) *J. Clin. Invest.* **117,** 3952–3957
50. Hayes, G. M., Carrigan, P. E., and Miller, L. J. (2007) *Cancer Res.* **67,** 2072–2080
51. Hayes, G. M., Carrigan, P. E., Beck, A. M., and Miller, L. J. (2006) *Cancer Res.* **66,** 3819–3827
52. Jang, S. W., Yang, S. J., Ehlén, A., Dong, S., Khoury, H., Chen, J., Persson, J. L., and Ye, K. (2008) *Cancer Res.* **68,** 4559–4570
53. Colwill, K., Feng, L. L., Yeakley, J. M., Gish, G. D., Cáceres, J. F., Pawson, T., and Fu, X. D. (1996) *J. Biol. Chem.* **271,** 24569–24575

Published online 3 September 2009

Nucleic Acids Research, 2009, Vol. 37, No. 19 6515–6527
doi:10.1093/nar/gkp633

Herpesvirus protein ICP27 switches PML isoform by altering mRNA splicing

Takayuki Nojima[1,2], Takako Oshiro-Ideue[1], Hiroto Nakanoya[1], Hidenobu Kawamura[1], Tomomi Morimoto[3], Yasushi Kawaguchi[3], Naoyuki Kataoka[4] and Masatoshi Hagiwara[1,2,*]

[1]Laboratory of Gene Expression, School of Biomedical Science, [2]Department of Functional Genomics, Tokyo Medical and Dental University, Yushima 1-5-45, Bunkyo-ku, Tokyo 113-8510, [3]Department of Infectious Disease Control, International Research Center for Infectious Diseases, The Institute of Medical Science, The University of Tokyo, Shirokanedai 4-6-1, Minato-ku, Tokyo 108-8639, Japan and [4]Medical Top Track (MTT) Program, Medical Research Institute, Tokyo Medical and Dental University, Yushima 1-5-45, Bunkyo-ku, Tokyo 113-8510

Received April 30, 2009; Revised July 6, 2009; Accepted July 16, 2009

ABSTRACT

Viruses use alternative splicing to produce a broad series of proteins from small genomes by utilizing the cellular splicing machinery. Since viruses use cellular RNA binding proteins for viral RNA processing, it is presumable that the splicing of cellular pre-mRNAs is affected by viral infection. Here, we showed that herpes simplex virus type 2 (HSV-2) modifies the expression of promyelocytic leukemia (PML) isoforms by altering pre-mRNA splicing. Using a newly developed virus-sensitive splicing reporter, we identified the viral protein ICP27 as an alternative splicing regulator of PML isoforms. ICP27 was found to bind preferentially to PML pre-mRNA and directly inhibit the removal of PML intron 7a *in vitro*. Moreover, we demonstrated that ICP27 functions as a splicing silencer at the 3′ splice site of the PML intron 7a. The switching of PML isoform from PML-II to PML-V as induced by ICP27 affected HSV-2 replication, suggesting that the viral protein modulates the splicing code of cellular pre-mRNA(s) governing virus propagation.

INTRODUCTION

As many as two-third of human genes produce two or more isoforms from one gene by alternative pre-mRNA splicing (1,2). Alternative splicing is strictly regulated across cell and tissue types, sex determinations, signal-regulated changes and developmental stages to provide a variety of gene functions depending on the situation (3,4). Alternative splicing also contributes to viral proteomic diversity (5). In the case of human immunodeficiency virus type 1, primary RNA transcripts are alternatively spliced to generate more than 40 different mRNAs (6). As viral RNA processing is often catalyzed by cellular RNA-binding proteins such as serine–arginine rich (SR) proteins (7,8), virus infection sometimes affects the host RNA processing factor (9,10). However, the effects of viral proteins on cellular mRNA splicing have poorly been investigated.

Herpes simplex virus type 2 (HSV-2) is a nuclear replicating DNA virus and a highly adapted human pathogen with rapid lytic replication cycle. When the viral capsid makes its entry into the host cell nucleus, HSV-2 genome DNA localizes to discrete nuclear foci called promyelocytic leukemia nuclear bodies (PML-NBs), also known as nuclear domain 10 (ND10) or PML oncogenic domain (POD) (11). PML was originally characterized as part of a fusion protein with RARα cloned from acute PML patients (12–14). PML is expressed in all normal tissues as well as tumor cell lines; however, its expression is reduced in some progressed tumors (15). The size of PML-NBs varies from 0.2 to 1 μm, and their frequency depends on cell type, cycle, and status (16–19). PML-NBs consist of many kinds of proteins involved in various functions (20,21), and are implicated in various cell processes, including apoptosis, DNA repair, transcription, senescence, cell proliferation, signal transduction and viral pathogenicity (19,20,22–29). PML-NBs have been thought to contribute to intrinsic antiviral defense on the interferon pathway (30). However, recent reports have indicated that PML-NBs provide scaffolds for DNA viruses and promote efficient viral propagation (11,24,31). Thus, a simple model is not sufficient to accommodate all accumulated evidence.

The human *PML* gene consists of nine major exons, and several alternatively spliced PML transcripts lead to

*To whom correspondence should be addressed. Tel: +81 3 5803 5836; Fax: +81 3 5803 5853; Email: m.hagiwara.end@mri.tmd.ac.jp

the expression of a multitude of different PML isoforms (32,33), as shown in Figure 1A. PML exon 1 to exon 4, which are common to all isoforms, are translated into the tripartite motif (TRIM) including the RING finger, B-box and coiled-coil domain. On the other hand, PML exon 5 to exon 9 can be alternatively spliced, generating multiple PML isoforms such as PML-I containing the putative exonuclease III domain (34). Furthermore, PML exon 6 contains the nuclear localization signal, and can be excluded for the expression of the cytoplasmic PML-VII isoform, which is essential for TGF-β signaling (27,33). Thus, the *PML* gene utilizes alternative pre-mRNA splicing for the functional diversity of its own protein products.

In this study, we hypothesized that the conflicting host–virus interactions at PML-NBs may reflect the differential functions of PML isoforms. Consequently, we found that the expression of PML splicing isoforms was switched during HSV-2 infection by alternative splicing. Our group has recently developed a splicing reporter capable of visualization of alternative splicing events *in vivo* and has also identified novel *trans*-acting factors (35,36). Here, we newly developed a virus-sensitive splicing reporter whose fluorescent protein expression is changed in HSV-2-infected cells, and we identified infected cell protein 27 (ICP27) as an alternative splicing regulator. ICP27 preferentially interacted with PML pre-mRNA and suppressed intron 7a removal presumably by modulating 3′ splice site (ss) recognition of the cellular *trans*-acting factor.

MATERIALS AND METHODS

Construction of plasmids

We constructed the reporter minigene PML E6-7b by amplifying the *PML* genomic DNA fragments spanning from exon 6 to exon 7b and cloning to a pcDNA3 vector (Invitrogen). Constructs expressing myc-tagged HSV-2 cDNAs and Flag-tagged ICP27 were prepared by inserting PCR products from the cDNA of HSV-2-infected HEK293 cells into the pcDNA3 vector. A construct for the preparation of the T-REx293/Flag-ICP27 stable cell line was prepared by inserting PCR products from the cDNA of HSV-2-infected HEK293 cells into the pcDNA5/FRT vector in accordance with the manufacturer's protocol (Invitrogen). Constructs expressing RFP-PML-II and RFP-PML-V were prepared by inserting PCR products from the cDNA of HEK293 cells into the pmRFP-C1 vector (Clontech). The constructs of ICP27 mutant M15, PML-small interference (siRNA)-resistant mutants, PML intron 7a-deletion mutant d1 and PML 3′ ss mutants m1-m4 were made using a QuikChange II XL kit (Stratagene). The cloning primers are shown in Supplementary Table S1.

RT–PCR

RNA was isolated from intact, HSV-2-infected cells, and transfected cells with sepasol RNA I (Nacalai). For reverse transcription, 500 ng of total RNA from each sample was incubated with oligo $(dT)_{20}$ and Superscript II reverse transcriptase (Invitrogen). PCR products were analyzed by 2% agarose gel electrophoresis, followed by ethidium bromide staining. As shown in Figure 1C, semi-quantitative PCR products were analyzed using the 2100 Bioanalyzer (Agilent Technologies) following the protocol stated in the manuals. The PCR primers are shown in Supplementary Table S2.

Viruses and antibodies

HSV-2 strain G [HSV-2 (G)] and Venus-HSV-2 strain YK381 were used at multiplicities of infection (MOI) based on their plaque-forming unit titers in Vero cells. Anti-Flag M2 antibody, anti-c-myc antibody, anti-ICP27 (8.F.137B) and Pan-PML antibody (H-238) were purchased from Sigma, Nacalai, Abcam and Santa Cruz, respectively. PML-II- and PML-V-specific sera were a kind gift from H. de The (18).

Construction of YK381 expressing Venus fluorescent protein

In pRB5198 (37), a region containing the bidirectional polyadenylation [poly(A)] signals of HSV-1(F) UL21 and UL22 was cloned into pBluescript II KS(+) (Stratagene). To construct p26.5-Venus, a SacI-BstEII fragment of pRB4090 (a kind gift from Dr Bernard Roizman) containing the promoter region of HSV-1(F) UL26.5 and a BamHI–EcoRI fragment of Venus/pCS2 (38) containing the entire open reading frame of Venus were subsequently cloned into pRB5198. The resultant plasmid contains a Venus expression cassette driven by the UL26.5 promoter. The BamHI fragment, 8.2 kb, encoding UL1 to a part of UL5 of the HSV-2 186 viral genome was cloned into pBluescript II KS(+) to yield p2UL3-4. p2UL3-4pac, in which the PacI site was introduced into the region between poly (A) signals for HSV-2 186 UL3 and UL4 genes, was generated by site-specific mutagenesis. p26.5-Venus in 2UL3-4 was constructed by cloning the SacI–KpnI fragment of p26.5-Venus containing the Venus expression cassette into the PacI site of p2UL3-4pac and used as a transfer plasmid for the generation of a recombinant virus YK381 expressing Venus fluorescent protein driven by the UL26.5 promoter, as described previously (38). YK381 exhibits an identical phenotype to wild-type HSV-2 186 in cell cultures and mouse models (T.M. and Y.K., unpublished observation).

Virus infection

HeLa and HEK293 cells were seeded into 6-well plates, and cells reaching 100% confluence were infected with HSV-2(G), as stated in the relevant figure legend. To examine the role of PML in HSV-2 replication, HeLa cells were transfected with PML siRNA for 48 h before the viral infection. For the PML splicing isoform rescue experiments shown in Figure 8F, HeLa cells were transfected with PML siRNA and then with plasmids containing either the siRNA-resistant RFP-PML-II mutant or RFP-PML-V mutant on the next day. HeLa cells were infected with HSV-2(G) for 24 h after plasmid transfection. The production of infectious HSV-2 was assessed by plaque assay in Vero cells (39). Vero cells